DIGITAL

INTEGRAL PROPORTIONAL CONTROLLER FOR DC

MOTORS

by

Sedat Nazlıbilek

B.S. in E.E., Boğaziçi University, 1982

Submitted to the Institute for Graduate Studies in Science and Engineering in partial fulfillment of the requirements for the degree of

Master of Science

in

Electrical Engineering

Boğaziçi University

1984

DIGITAL INTEGRAL PROPORTIONAL CONTROLLER FOR DC MOTORS

APPROVED BY

Doç. Dr. Okyay KAYNAK Kaynak

(Thesis supervisor)

Dr. Ahmet DENKER

Dr. Oğuz TOSUN O. Tosun

DATE OF APPROVAL 23 Ağustos 1984

ACKNOWLEDGEMENT

This thesis has been prepared for the partial fulfillment of the requirement of Bosphorus University, School of Engineering, for the degree of Master of Science.

I wish to express my gratitude and sincere thanks to Doç. Dr. Okyay Kaynak, my thesis supervisor, for his kind interest and guidance in the accomplishment of this work.

TABLE OF CONTENTS

ABSTRACT

The object of this thesis is to analyse and design a microprocessor based digital speed control system for a d.c. motor system with an IP(Integral-Proportional) control algorithm. Also, the PI and the IP control systems are analysed using Laplace transforms and z-transforms in the case of analog and discrete cases respectively. They are compared according to speed control accuracy, stability, and especially load characteristics.

The experimental set-up comprises a dc motor driven by a three-phase fully controlled bridge. The firing angle of the bridge is directly controlled by the microcomputer. For the sensing of speed feedback signal, a dc tachogenerator with a ten-bit A/D converter is utilised.

The equations of the system are derived in discrete form and by use of them , it is shown that IP control resul in a better performance than that of the PI control especially with respect to changes in the load torque.

ÖZETÇE

Bu tez çalışmasının konusu tümlevsel-oransal denetimli bir d.a. motorunun hız denetiminin mikroişlemci kullanılarak tasarımlanması ve analizinin yapılmasıdır. Aynı zamanda , oransal-tümlevsel ve tümlevsel-oransal denetim dizgelerinin analog ve diskret(ayrık) analizleri sırasıyla Laplace-dönüşümleri ve z-dönüşümleri vasıtasıyla yapılmıştır. Bu iki dizge hız denetim doğruluğu, kararlılık, ve yüklenme durumlarına göre biribirleriyle kıyaslanmışlardır.

Deneysel dizge, üç-evre tam denetimli köprü ile sürülen bir da motorundan ibarettir. Köprünün tetikleme açısı mikroişlemci tarafından doğrudan denetlenmektedir. Geribesleme imi bir takoüretece bağlı bir on-bit A/D dönüştürücü ile sağlanmaktadır.

Dizge denklemleri ayrık(discrete) halde türetilmiştir. Tümlevsel-oransal denetimin sonuçlarının oransal-tümlevsel denetimden daha iyi olduğu görülmüştür. Özellikle yüklenme durumunda tümlevsel-oransal dizge daha iyi bir performans göstermektedir.

LIST OF FIGURES

LIST OF TABLES

LIST OF SYMBOLS

α .... Firing angle

β .... Integration result

τ .... Time variable

τ_m .... Motor mechanical time constant

λ .... Eigenvalue

ξ .... Damping factor

τ_e .... Electrical time constant

V_τ .... load disturbance

ϕ .... STM (State transition matrix)

I. DESIGN OF CONTROL SYSTEMS

A. Introduction

A control system is composed of a physical system and controllers which are designed such that it utilises the desired performance of the physical system. A well designed control system must satisfy the following characteristics:

(A) system must be stable;

(B) system must be robust,

(C) the effects of undesirable inputs such as noise, load disturbance ect. to outputs must be as small as possible,

(D) the outputs must track the inputs as close as possible.

It is impossible to satisfy all of thse characteristics for a physical system, or it requires complex and expensive controllers.

For usual design methods, either time-domain criterians like overshoot, steady-state error, rise-time, settling time, or frequency domain criterians like phase, gain, bandwidth are examined. In fact, with respect to the system performance, the behaviour of the system in the time-domain is important, that is in our case, the response of the system to a step input. Therefore, time-domain criterians are the actual response criterians of the system.

In some cases, we can reach the design aims by changing some parameters of the system. However, in most cases, this is impossible. Therefore, in this case, we introduce some controllers to a closed loop system. Controllers can be placed anywhere in the closed loop.

Recent advances in LSI technology has awakened a new interest in digital control of motor drive systems. The application of microprocessors enlarges the selection range of control algoritms and increases the performance of drive systems considerably. The establishment of a guide line is necessary to select a suitable control algoritm for a particular design requirement.

For the evaluation of the performance of a motor control system, as we mentioned, the accuracy, the speed of response and the sensitivity of the system can be considered as primary indices. In figure 1.A.1 several control algoritms of motor drives are classified according to accuracy, response and robustness. The PI control is a conventional method and widely used in industrial applications. The PLL control system gives more precise speed accuracy than that of the PI control system(1). With respect to dynamic response, however, the speed settling time of a PLL controlled motor is very long since it is based on integral control. The minimum-time settling control achieves very fast response when the system configuration is optimally designed to achieve the deadbeat response(2). The minimum-time settling control system is a very high gain feedback control system so the performance of this system is sensitive to the deviation of motor parameters. The sliding mode control is introduced to obtain a robust control performance to the parameter deviation and/or the load torque disturbances(3). Robustness, in other words low sensitivity to deviations in the motor parameters, is a very important index in industrial applications but unfortunately is sometimes neglcted in the design stage.

We introduce a method to design a microprocessor-based digital speed control system taking into account the above mentioned indices. It is an Integral-Proportional(IP) control, which will be discussed later and is different from the conventional PI control law, giving a fast response.

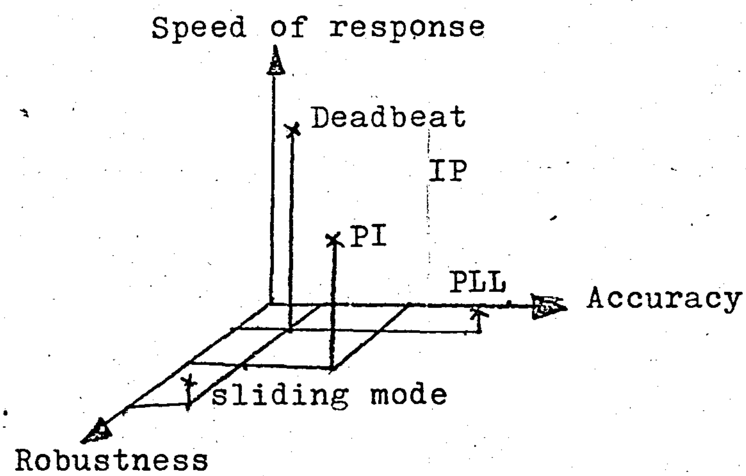

Fig.1.A.1 Perfórmance evaluation of control algorithm of motor drive.

B. The Design Methods and Types of Controllers

At the design stage of a system, designers use some methods. The most common method is the root locus method.

The basic characteristic of the transient response of a closed loop system is determined from the closed loop poles. Thus, in analysis problems, it is important to locate the closed loop poles in the s-plane. In the design of closed loop systems, we want to adjust the open loop poles and zeroes at desirable locations in the s-plane.

The closed loop poles are the roots of the characteristic equation. Finding them requires factoring the characteristic polynomial. That is, in general, laborious if the degree of the characteristic polynomial is three or higher. The classical techniques of factoring polynomials are not convenient because as the gain of the open loop transfer function varies, the computations must be repeated

A simple method for finding the roots of the characteristic equation has been developed by W.R. Evans and used extensively in control engineering. This method, called the root locus method, is one which the roots of the characteristic equation are plotted for all values of a system parameter. The roots corresponding to a particular value of this parameter can then be located on the resulting graph. Note that the parameter is usually the gain but any other variable of the open loop transfer function may be used.

Root locus gives a lot of information about the the time response and the frequency response of the system. Therefore, this method is more useful than the others.

There are many types of controllers. The most commonly used methods are proportional controllers, proportional-integral controllers, proportional-derivative controllers, and proportional-integral-derivative controllers. The method we will use is another type of controller which is called Integral-Proportional (IP) controller. The difference between the conventional PI and IP controllers is that in IP control system, the proportional term is moved from forward loop to the feedback loop.

C. The Effects of Poles and Zeros to the Transient Response

Now we will discuss a system in general. We will introduce some poles and zeros to the system transfer function, and observe the effect of them to the transient response and also system parameters of the system.

In general, a control system transfer function in Laplace domain can be represented as follows:

$$G(s)= \frac{Kz(s)}{p(s)}$$

If the system is a first order system, then

$$G(s)= \frac{K}{s+b}$$

there is only one pole in the s-plane. In the time domain, the response of the system is

$$Y(s)= \frac{K}{s(s+b)} = \frac{K/b}{s} - \frac{K/b}{s+b}$$

$$y(t)= \frac{K}{b} - \frac{K}{b}\exp(-bt)$$

This output can be drawn as shown in fig. 1.C.1

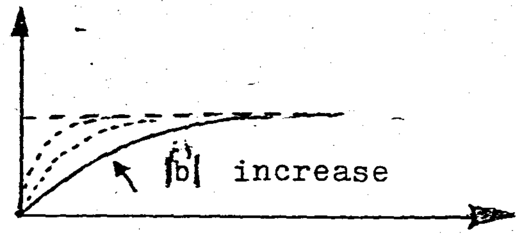

Fig.1.C.1 Output of the first order system.

If the absolute value of the pole is increased, we would see that the step response would be fast but steady state value would be small, therefore K must be increased.

Let's introduce another pole to the above system transfer function. Then

$$G(s)= \frac{K}{(s+a)(s+b)}$$

The step response of that system is

$$Y(s)= \frac{K}{s(s+a)(s+b)} = \frac{K/ab}{s} + \frac{K/a(a-b)}{s+a} - \frac{K/b(a-b)}{s+b}$$

$$y(t)= \frac{K}{ab} + \frac{K}{a(a-b)} \exp(-at) - \frac{K}{b(a-b)} \exp(-bt)$$

If $a < b$

$$y(t)= \frac{K}{ab} - \frac{K}{a|a-b|} \exp(-at) + \frac{K}{b|a-b|} \exp(-bt)$$

$$y(t) = \frac{K}{ab} - \frac{K}{a\alpha}\exp(-at) + \frac{K}{b\alpha}\exp(-bt)$$

where $\alpha = |a-b|$ then

$$\frac{K}{a\alpha} > \frac{K}{b\alpha}$$

the unit step response is shown in fig.1.C.2

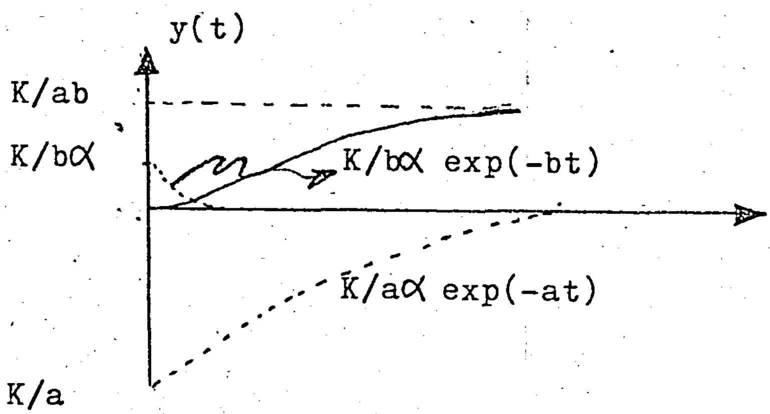

Fig.1.C.2 Unit stepresponse of the second order system when $a < b$

Now we introduce a zero to the same system

$$G(s) = \frac{K(s+c)}{(s+a)(s+b)}$$

the step response is

$$y(t) = \frac{Kc}{ab} + \frac{K(-a+c)}{-a(-a+b)}\exp(-at) - \frac{K(-b+c)}{b(-b+a)}\exp(-bt$$

The values of K, c, a will effect the step response of the system. There may be some different cases like c<a<b, c=a<b, c>a<b etc. In every case, the step response will be different. There may be an overshoot, slow response etc.

In the case of c=a b, there is a cancelation between zero and the pole, and the step response is like in Fig.1.C.1.

In Fig.1.C.3 there are some step responses corresponding to the different parameter values. From these figures and mathematical equations we conclude some important results that will be very useful when we examine the practical control system.

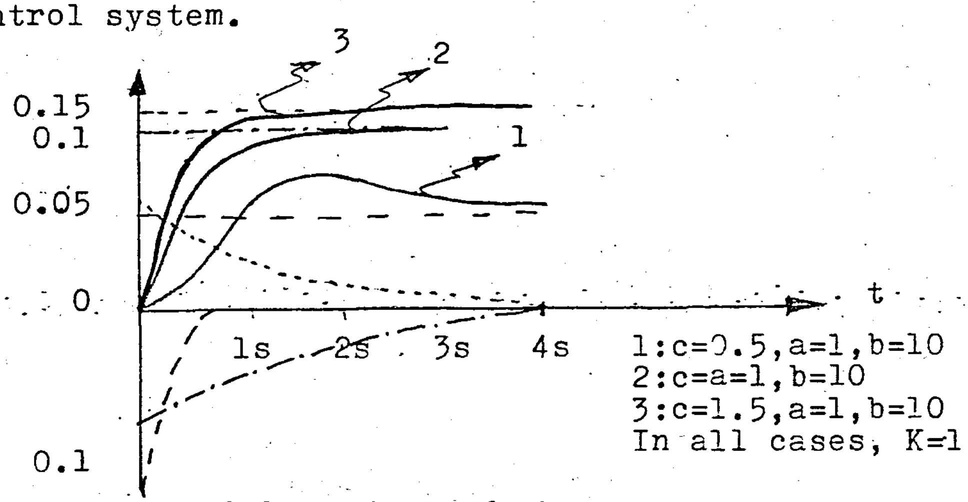

Fig.1.C.3 Effect of the zero.

The results of this analysis is that:

(A) when the value of the zero decreases, and comes to the right of the pole which results in slow response, there would be an overshoot. Also the steady-state value would decrease;

(B) when the value of the zero increase, the overshoot would disappear, steady-state value would increase, but the response would be slow.

In fact, the zero closest to the imaginary axis causes the highest overshoots.

II. THE PI CONTROL SYSTEM AND THE IP CONTROL SYSTEM

A. The PI Control System

The Proportional-Integral controller is used to eliminate the steady-state error and increase the response of a closed loop system.

In the integral control of the plant, the control signal, the output signal from the controller, at any instant is the area under the actuating error signal curve upto that instant. The control signal u(t) can have nonzero value when the actuating error signal e(t) is zero, as shown in Figure (a) This is impossible in the case of the proportional controller since a nonzero control signal requires a nonzero actuating error signal. (A nonzero actuating error signal at steady state means that there is an offset). Figure (b) shows the curve e(t) versus t and the corresponding curve u(t) versus t when the controller is of the proportional type.

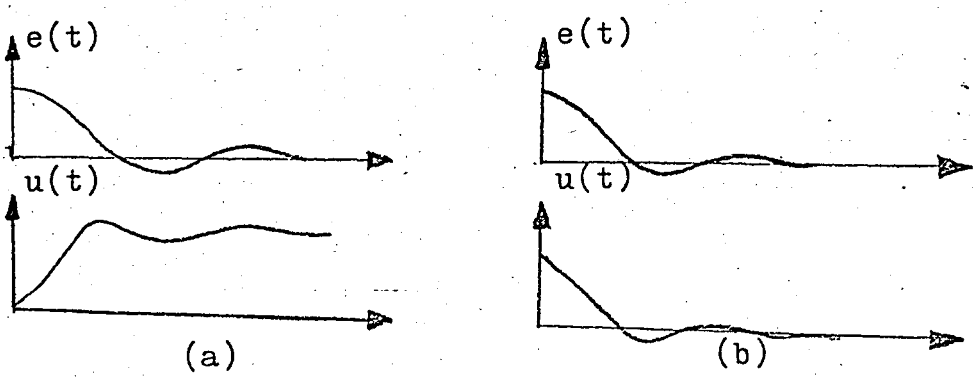

Fig.2.A.1 (a) Plots of e(t) and u(t) curves showing nonzero control signal when the actuating error signal is zero; (b) plots of e(t) and u(t) curves showing zero control signal when the actuating error signal is zero

— Note that integral control action, while removing offset or steady-state error may lead to oscillatory response of slowly decreasing amplitude or even increasing amplitude, both of which are usually undesirable.

Let us now control a physical system which has a transfer function

$$G(s)=\frac{Km}{1+sTm}$$

by applying the Proportional-plus-Integral control. Proportional-plus-Integral controller has a transfer function of

$$G_{pi}(s)=\frac{Ki}{s}+Kp$$

The block diagram of a PI control system is shown in Figure 2.A.2 where V_{τ} is the load disturbance

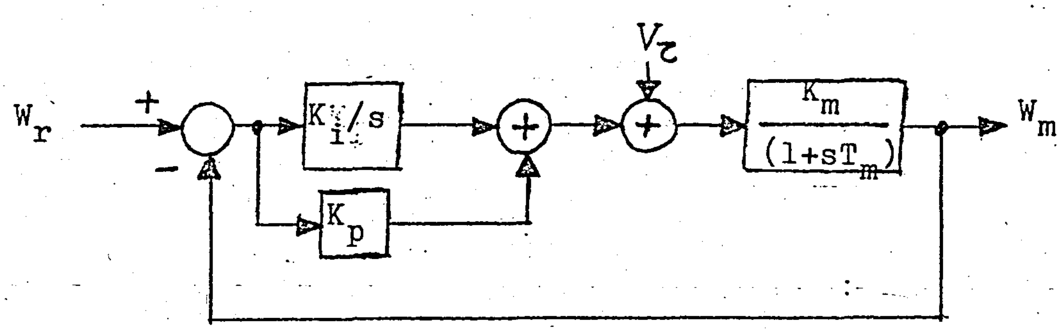

Fig.2.A.2 Block diagram of PI control system.

Now, we will derive the overall transfer function Wm/Wr first, secondly Wm/V_c, and open-loop transfer function.

$$\frac{Wm(s)}{Wr(s)} = \frac{(Ki/s+Kp)Km/(1+sTm)}{1+(Ki/s+Kp)Km/(1+sTm)}$$

$$= \frac{(Ki/s+Kp)Km}{1+sTm+(Ki/s+Kp)Km}$$

$$= \frac{KiKm+sKpKm}{Tms^2+(1+KpKm)s+KiKm}$$

$$\frac{Wm(s)}{Wr(s)} = \frac{KiKm(1+sKp/Ki)/Tm}{s^2+s(1+KpKm)/Tm+KiKm/Tm}$$

The transfer function between the actuating error signal e(t) and the input signal $w_r(t)$ is

$$\frac{E(s)}{Wr(s)} = 1-\frac{Wm(s)H(s)}{WWr(s)} = \frac{1}{1+G(s)H(s)}$$

$$= \frac{1}{1+G(s)} = \frac{1}{1+(Ki/s+Kp)(Km/(1+sTm))}$$

using the final value theorem

$$e_{ss} = \lim_{t \to \infty} e(t) = \lim_{s \to o} sE(s)$$

$$= \lim_{s \to o} \frac{sWr(s)}{1+G(s)}$$

since $W_r(s) = 1/s$ (unit step)

$$e_{ss} = \lim_{s \to o} \frac{1}{1+(K_i/s+K_p)(K_m/(1+sT_m))}$$

$$e_{ss} = 0$$

As it can be seen, the steady- state error is zero.

If we consider that the input will not change, the the effect of the load torque disturbance is observed from Figure. 2.A.3

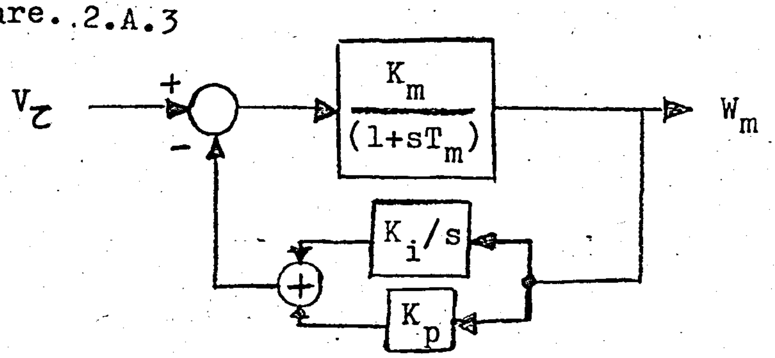

Fig.2.A.3 The transfer block diagram between the output and the load change input.

$$W_m = \frac{K_m/(1+sT_m)}{1+(K_i/s+K_p)K_m/(1+sT_m)} V_\tau$$

$$= \frac{K_m s}{s^2 T_m + s(1+K_m K_p) + K_i K_m}$$

$$W_m/V_\tau = \frac{s K_m / T_m}{s^2 + s(1+K_p K_m)/T_m + K_i K_m / T_m}$$

The open-loop transfer function of the PI control system can be obtained as follows,

$$G(s)H(s) = G_{ol}(s) = K_m(K_i/s + K_p)/(1+sT_m)$$

$$= (K_i K_m + sK_p K_m)/(s^2 T_m + s)$$

$$G_{ol}(s) = \frac{K_m K_p (s + K_i/K_p)/T_m}{s(s+1/T_m)}$$

B. The IP Control System

The IP control system is actually based on the state-vector feedback theory. The block diagram of the IP control system is different from the PI control system, since the proportional term is moved to feedback loop from forward loop. The block diagram of the system controlling the same plant used in the PI control is shown in Figure.2.B.1

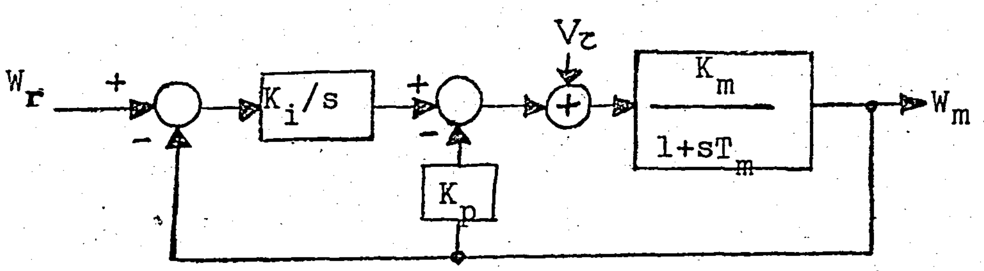

Fig.2.B.1 Block diagram of the IP control system

The overall transfer function can be derived from the blok diagram.

$$W_m = \frac{K_m}{1+sT_m}\left((W_r - W_m)K_i/s - K_p W_m\right)$$

$$W_r \frac{K_i K_m}{s(1+sT_m)} = W_m\left(1+K_i K_m/s(1+sT_m)+K_p K_m/(1+sT_m)\right)$$

$$W_m/W_r = \frac{K_i K_m}{s^2 T_m + s(1+K_p K_m) + K_i K_m}$$

$$W_m/W_r = \frac{K_iK_m/T_m}{s^2+s(1+K_pK_m)/T_m+K_iK_m/T_m}$$

As we can see from the block diagram(Fig.2.B.1) the output to load disturbance transfer function of the IP control system is the same as the PI control system. That is,

$$W_m/V_\tau = \frac{sK_m/T_m}{s^2+s(1+K_mK_p)/T_m+K_iK_m/T_m}$$

The open-loop transfer function of the IP control system can be derived as follows:

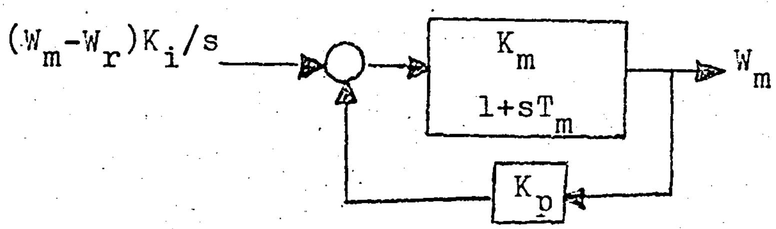

$$\frac{W_m}{K_i(W_r-W_m)/s} = \frac{K_m}{1+K_mK_p+sT_m}$$

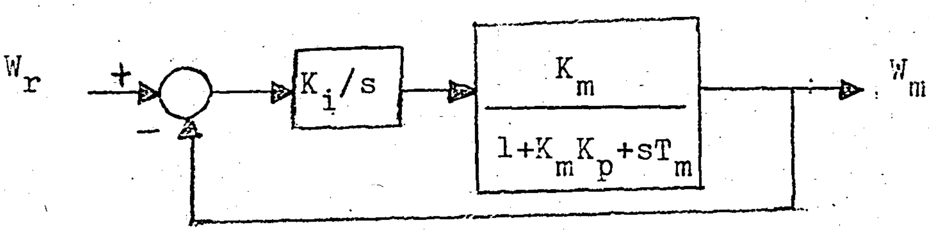

$$W_m/W_r = \frac{K_i K_m/T_m}{s^2+s(1+K_p K_m)/T_m+K_i K_m/T_m}$$

or

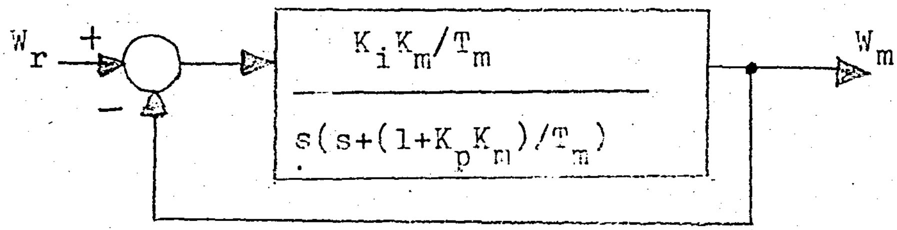

$$G(s)H(s) = \frac{K_i K_m/T_m}{s(s+(1+K_m K_p)/T_m)}$$

C. The Comparison of the PI and the IP Control Systems

In Table.1 , both the PI and the IP control system transfer fuctions are shown

TABLE. 1

PI	IP	
$\frac{W_m(s)}{W_r(s)} = \frac{K_i K_m/T_m(1+sK_p/K_i)}{G_o(s)}$	$\frac{K_i K_m/T_m}{G_o(s)}$	overall closed loop transfer function
$\frac{W_m(s)}{V_{\tau}(s)} = \frac{sK_m/T_m}{G_o(s)}$	$\frac{sK_m/T_m}{G_o(s)}$	load torque transfer function
$G(s)H(s) = \frac{K_m K_p(s+K_i/K_p)/T_m}{s(s+1/T_m)}$	$\frac{K_i K_m/T_m}{s(s+(1+K_m K_p)/T_m)}$	open loop transfer function

where $G_o(s)=s^2+s(1+K_p K_m)/T_m+K_i K_m/T_m$

From the above equations, it is seen that there is one important difference between the PI and the IP control systems. In the overall transfer function of the PI control system, there is a zero, eventhough the poles of both system are the same. The effects of this zero will be investigated. The PI and the IP control systems have the same load torque transfer funtion. There is a zero at the origin of W_m/V_τ resulting in zero steady-state speed change. Using the final value theorem, it can easily be proved as follows,

$$\lim_{s \to 0} sW_m(s) = \lim_{s \to 0} s \frac{s\, K_m/T_m}{s^2+s(1+K_pK_m)/T_m+K_iK_m/T_m} \cdot \frac{1}{s}$$

$$= 0$$

Let us show the IP control system in block diagram form(Fig.2.C.1). This system is of the form like in Figure.

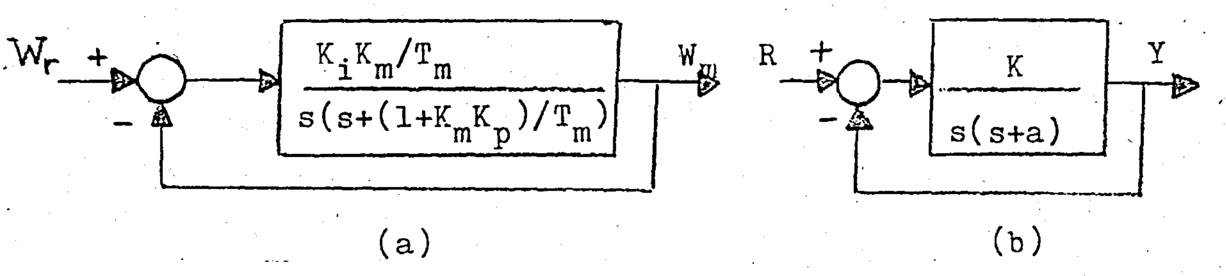

Fig.2.C.1 Block diagram of the IP control system

Root locus of the IP control system is shown in Figure.2.C.2

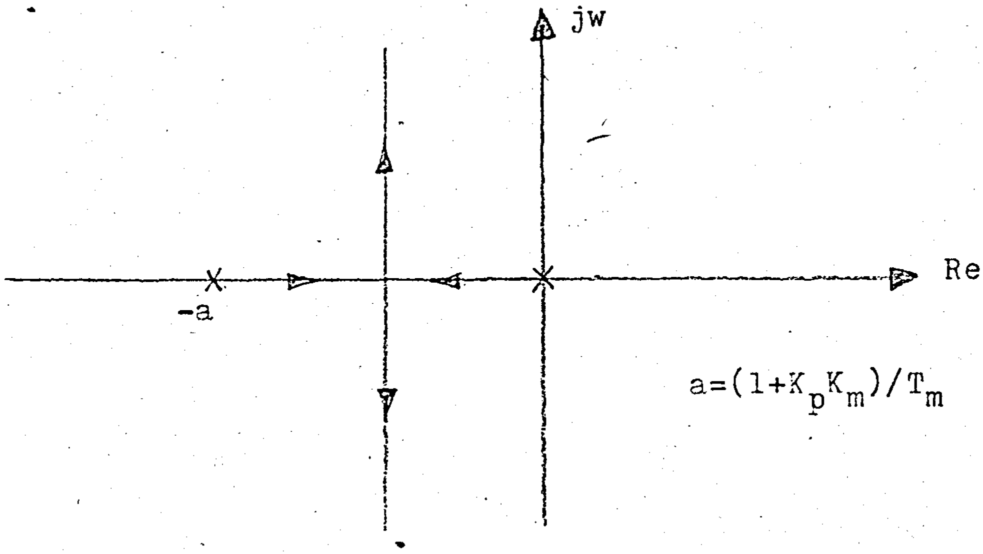

Fig.2.C.2 Root locus of the IP control system

When the value of K_p increase, it is expected that the response of the system will increase.

When the gain, K, of the system changes, the poles move on the graph in the directions of the arrows. In order to change the gain, we must change the value of the integral coefficient K_i . If we decrease the proportional coefficient K_p, the poles in 'a' will shift to the left and result in fast response. But in this case, the pole must not loose its dominant characteristic.

The closed-loop transfer function of the system shown in figure.2.C.1(b) is

$$Y(s)/R(s)= \frac{K}{s^2+as+K} = \frac{w_n^2}{s^2+2\zeta w_n s+w_n^2}$$

$$s_{1,2}= -a\mp\sqrt{a^2-4K/2} = -\zeta w_n \mp w_n\sqrt{\zeta^2-1}$$

$a^2 > 4K$ or $\zeta^2 > 1$ roots are real

$a^2 = 4K$ or $\zeta^2 = 1$ roots are equal

$a^2 < 4K$ or $\zeta^2 < 1$ riits are imaginary.

When the roots are real, in this case, as damping ratio ,ζ, approaches to 1, the system responds to a unit step more quickly. Therefore , we must increase the value of the integral coefficient K_i . The larger the value of K_i, the smaller the damping ratio ζ.

We said that if we gave large values for K_p, the response would have been faster. But, this is not a true approach in the case of the IP control system, because when the value of K_p is large, then the damping ratio will away from 1, that is, ζ gets large values. The value of K_p must be kept at a sufficient value.

In order to obtain a good response without overshoot, both 'K' and 'a' must be chosen large enough.

We experienced above discussion by a numerical example, where $K_m = 0.94$, $T_m = 0.46$, and $K_i = 2$, $K_p=2$; then $K_i = 10$, $K_p = 2$; and then $K_i = 30$, $K_p = 2$. The results are drawn in Figure 2.C.3. Notice that K_p is kept constant, and K_i is increased. But for a good response (quick and without overshoot) , we had chosen large K_i and K_p values ($K_i=60$, $K_p = 9$)and the output was drawn in Figure.2.C.4.

Conclusion is that, we can find such large K_i and K_p values that the response of the IP control system becomes fast without overshoot. The large parameter values also bring some important advantages in the case of load disturbances, which are explained later.

The Proportional-Integral control system has a

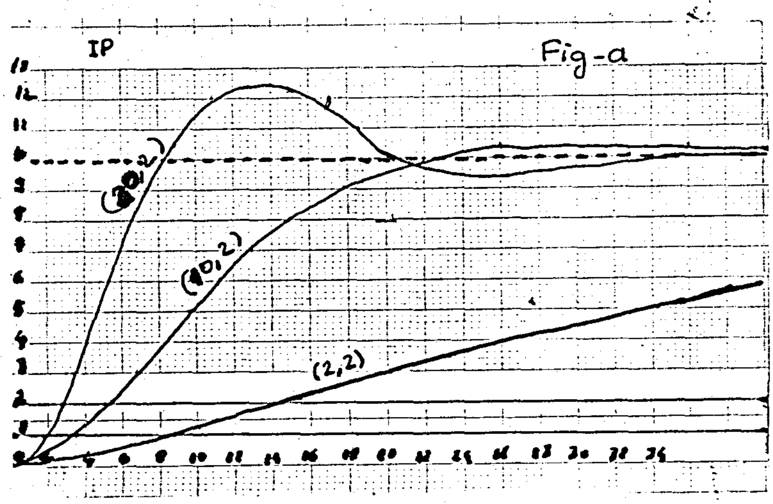

Fig.2.C.3 Results of the IP control for several parameters.

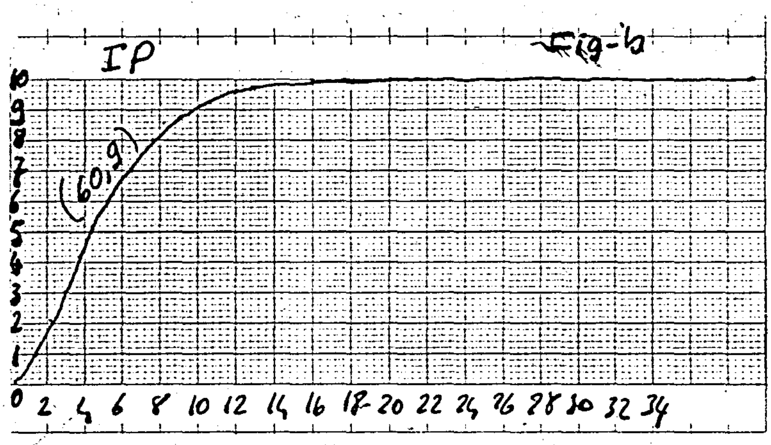

Fig.2.C.4 Step response of the IP without overshoot

block diagram shown in Figure 2.C.5

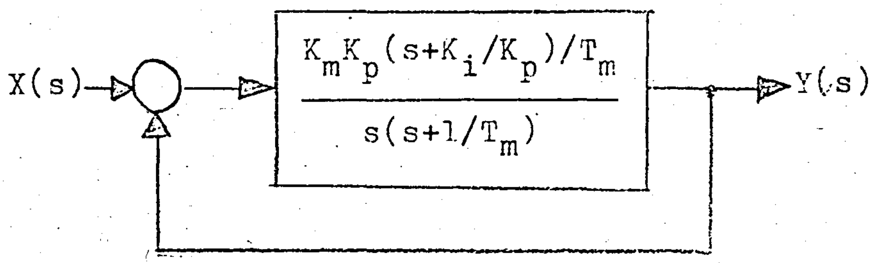

Fig.2.C.5 PI control system

The only difference from the IP control system is a zero in the transfer function of the PI control system The effect of this zero is explained.

When we give large values for K_i and K_p, it is expected that an overshoot will occur.

We know that the aim of introducing a zero to the transfer function of a PI control system is to cacel out the pole that results in slow response and to decrease the steady-state error. But for large values of parameters as in the case of the IP control system results in an overshoot in a PI control system, differ from the IP. As the value of K_p increase, the zero begins to shift to the right and comes to the right of the pole corresponding to slow response. Also, K_i value determines the places of the poles and the zero in the s-plane. The places of the poles and the zero are very important. Let's discuss some different cases:

$$G_{ol}(s)= \frac{K_m K_p (s+K_i/K_p)/T_m}{s(s+1/T_m)}$$

$$= \frac{K(s+a)}{s(s+1/T)}$$

where $a = K_i/K_p$, $K=K_m K_p/T_m$, $T=T_m$

From this transfer function, it is possible to draw two different root loci of the PI control system

(A) $|a| < |1/T|$

(B) $|a| > |1/T|$

Both of which are shown in Figure 2.C.6 respectively.

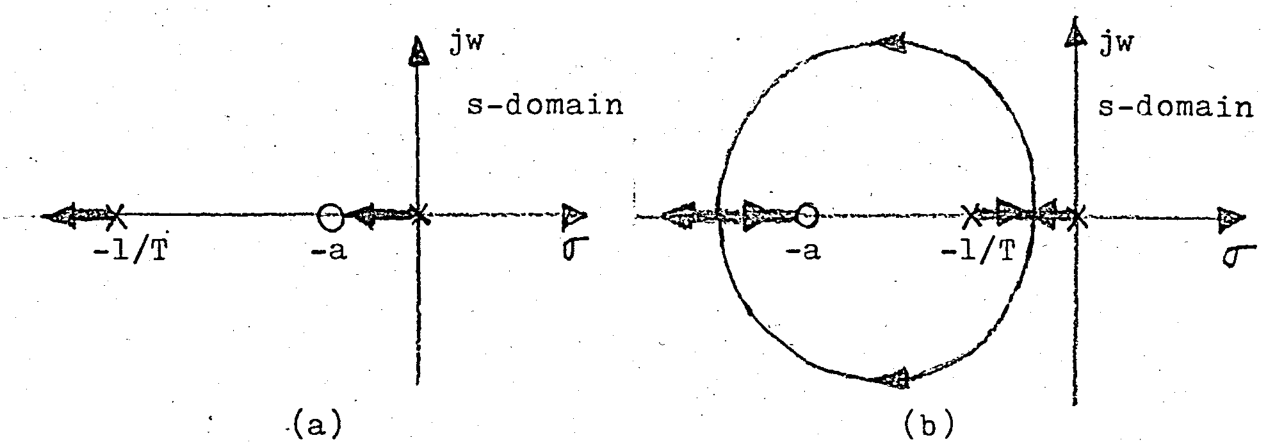

Fig.2.C.6 Root loci of the PI control system

In order to obtain the case (A), small K_i and K_p values must be chosen for practical purposes. In this case there would be no overshoot, but the response would be slow

In the second case, when the gain is increased, the poles will take complex values, and the oscillations will be observed. It is possible to stop the oscillations by means of very large gain, but then the poles will shift to the left of the zero, and an overshoot will always be observed. Also, for a very large gain, it is necessary to choose the values of K_i and K_p very large. This is not a practical solution. Three different situations; the zero is between the poles, the poles are complex, and the zero is at the right of the poles were examined and the results are shown in Figure.2.C.7a For each case, the places of the poles and the zero are shown in Fig.2.C.7b respectively.

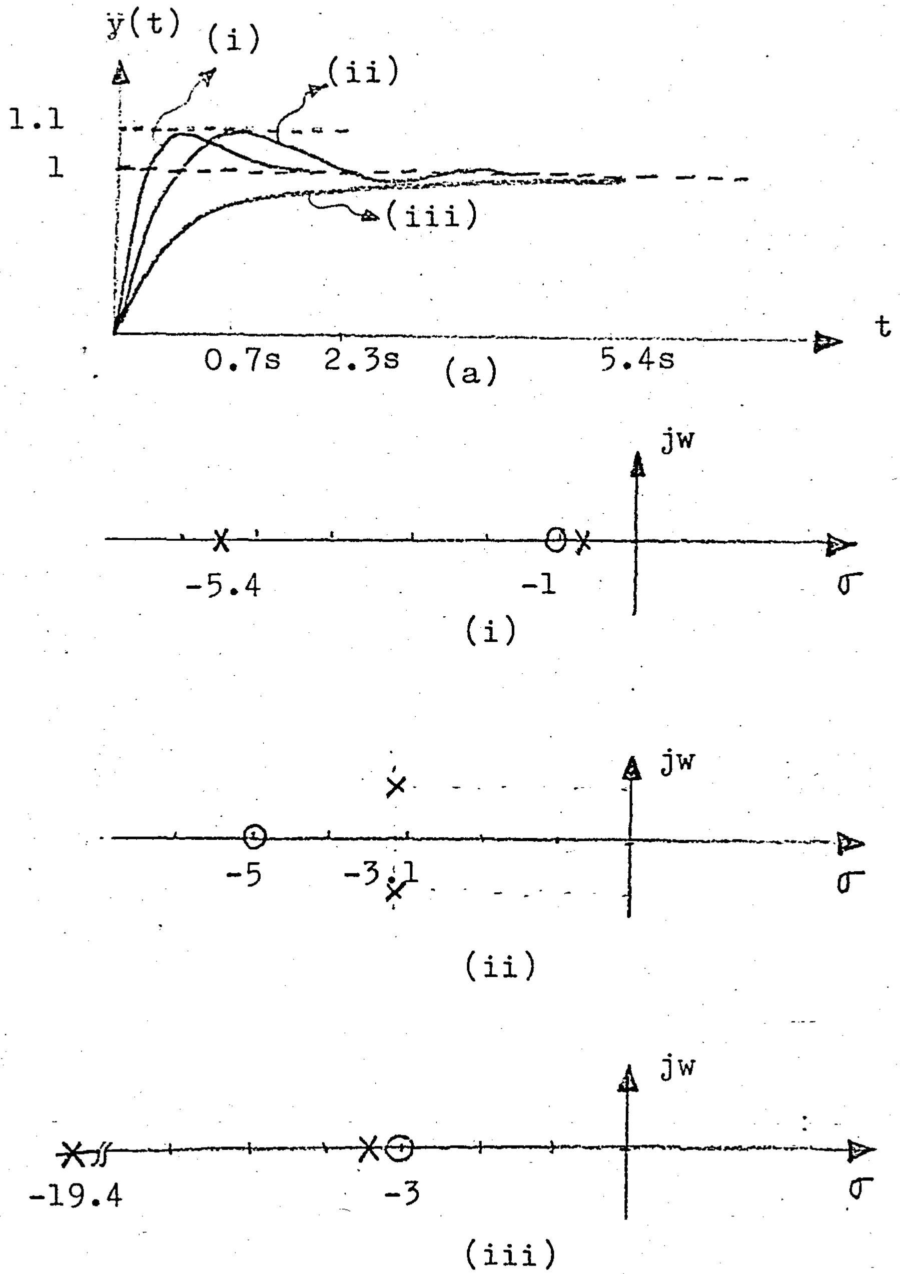

Fig.2.C.7 Step responses of the PI control system (i) the zero is between the poles;(ii) poles are complex;(iii) the zero is at the right of both pole.

D. Load Torque Disturbance

As we can see from table.1, both the PI and the IP control systems have the same load-to-output transfer function. Let's show this block diagram once more again in Figure.2.D.1

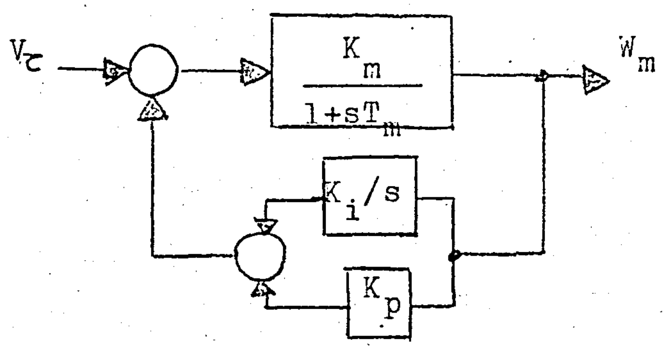

Fig.2.D.1 Load-to-speed block diagram of both PI and IP control systems.

The transfer function is

$$W_m/V_\tau = \frac{s\,K_m/T_m}{s^2+s(1+K_pK_m)/T_m+K_iK_m/T_m}$$

As we mentioned earlier, large parameter values give rise to an overshoot. Larger overshoot is the penalty for the shorter rise-time . The overshoot in the PI control system is undesirable since it requires a higher capacity of power converter. If we design a PI control system having large parameters in order to obtain fast response to a change of load, we can succeed it in a quickest manner, but in this case because of the overshoot we must use a high capacity power converter. It is possible to design the PI control system with no overshoot. However, in this case, the motor speed recovering time from the load disturbance is very long. We can explain this effect as follows, As we have seen, until some values of K_i and K_p, the zero and the pole representing the slow response of the PI control system are cancelled out each other. But this improves only the response to the reference speed but does not effect the response to a load disturbance.

This very serious problem, especially in the case where fast response is a main subject of the design, can be solved by another control algoritm, which is called IP control algoritm. Since the IP control system can take larger parameter values without overshoot, and these parameters are also necessary for load change response, it has better dynamic performance than that of the PI control system.

From Figure.2.D.2, we can see the responses to change of load. As seen, for large values, speed recovering time is smaller.

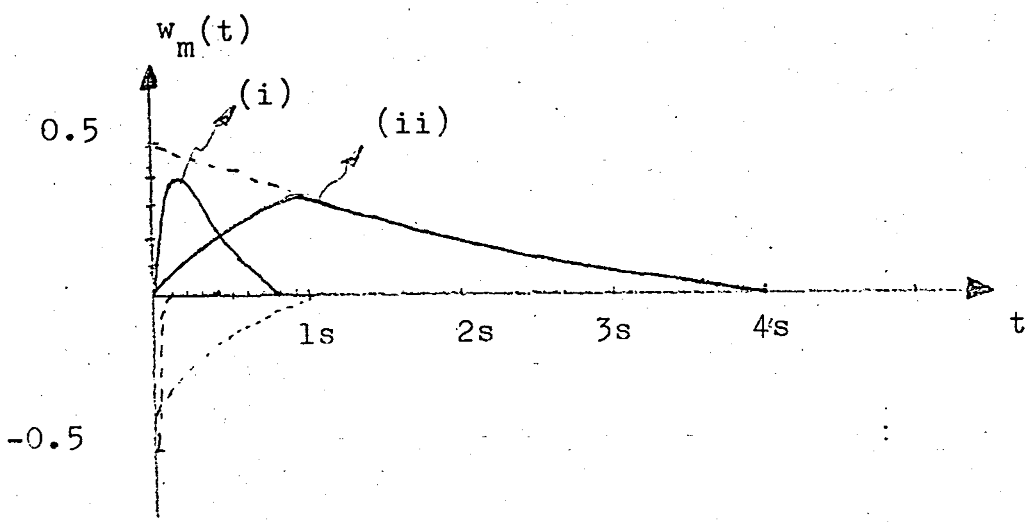

Fig.2.D.2 Change of the load.

III. DISCRETE IP CONTROL SYSTEM DESIGN

A. Introduction

Since the outputs of digital control systems are usually functions of the continuous variable t, it is necessary to evaluate the performance of the system in the time domain. However, when the z-transform or the discrete time state equation is used, the outputs of the system are measured only at the sampling instants. Depending on the sampling period and its relation to the time constants of the system, the discrete-time representation may or may not be accurate. In other words, there may be a large discrepency between the output c(t) and the sampled signal $c^*(t)$, so that the latter is not a valid representation of the system behaviour.

As in the studies of continuous-data control systems, the time response of a digital control system may be characterized by such terms as the overshoot, rise time, delay time, settling time, damping ratio, damping factor, natural undamped frequency etc.

The performance of a digital control system in the time domain is often measured by applying a test signal such as a unit-step function to the system input. For a linear system the unit-step input can provide valuable information on the transient and steady-state behaviour of the system. In fact, overshoot, rise time, delay time and settling time are all defined with respect to a unit-step input.

- When the z-transform or the discrete-time state equation is used for the analysis of digital control systems the system responses are represented only at the sampling instants. Care must be taken in judging on the accuracy and validity of these discrete-time data, as they may not be an accurate representation of the true responses of the digital system.

If the sampling period is sufficiently small, then the sampled response gives an adequate representation of the true response. However, in general, if the sampling period is too large, the sampled-data representation may be entirely erroneous. It should be pointed out that the selection of the sampling period of a digital system is usually not based on just the accuracy of representation of the system responses at the sampling instants, but more importantly on the overall system performance, stability, and hardware considerations.

The stability of linear feedback control systems depends predominantly on the gain of the control loop, on the poles and zeros of the controlled system, on the magnitude of transportation lags, and perhaps on several other less important physical characteristics. A criterian for the stability of continuous time systems consists of testing whether the eigenvalues of the system matrix or the closed-loop poles all have negative real parts. In the analysis of discrete-time systems one other important design parameter enters into the consideration of stability; this is, as we mentioned, the sampling period T.

Actually, a linear time-invariant discrete system is stable iff

i) $|\lambda_i| \leq 1$,

ii) If $|\lambda_i| = 1$ then λ_i is a root of multiplicity one in the minimal polynomial.

In reality, the system that we control is a microcomputer controlled dc motor control system. Since the microprocessor manages coded I/O data at a sampling instant and executes the control program during a sampling period, the motor control system operates actually as a sampled data system.

First of all, we will design the speed control system using Integral-Proportional (IP) controller. The roots of the characteristic equation represent the natural modes of the closed-loop system, however, the transient behaviour and the frequency response are strongly influenced by the location of the zeros.

For these reasons, first work that we will do is to apply root locus technique to a preliminary design, i.e to stabilize the system and to relocate the dominant poles at a desired position. Improvement of the closed-loop performance to achieve desired specifications is obtained using a digital simulation.

In the digital simulation of the dynamic system the programming of the solution of differential and/or difference equations is required. The digital machine performs its basic operations involving arithmetic, memory, and logic operations, in terms of variables which are always represented in discrete form. We must convert all continuous mathematical operations into a corresponding discrete form before they can be processed by the microcomputer.

Before the simulation, we can determine the controller parameters which are necessary for the desired response by using the root locus technique. Then using the discrete state equations of the system and the controller, we can simulate the system in the digital machine. Recursive equation of the controller is then programmed in the microcomputer in machine language and the actual system can be operated.

B. Comparison of Time Responses of Continuous-Data and Digital Control Systems

We will discuss the responses of continuous-data motor speed control system and the corresponding digital control system.

The block diagram of the motor speed control system is shown in Fig.3.B.1

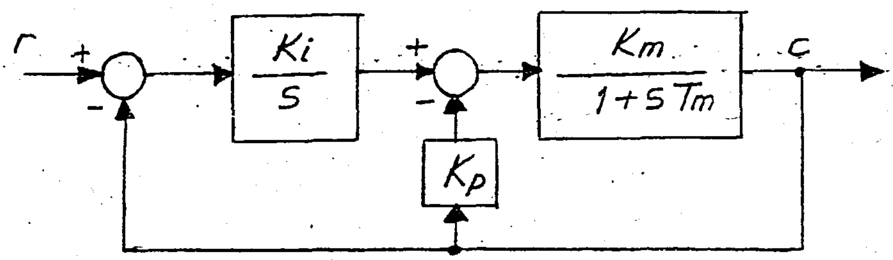

Fig.3.B.1 Continuous-data motor control system.

Closed-loop transfer function of the system can be written as

$$\frac{C(s)}{R(s)} = \frac{K_i K_m / T_m}{s^2 + s(1 + K_p K_m)/T_m + K_i K_m / T_m}$$

where

K_i=Integral coefficient=120

K_p=Proportional coefficient=9

K_m=Motor gain=0.94

T_m=Motor time constant=0.46

Substituting the system parameters, we have

$$\frac{C(s)}{R(s)} = \frac{245}{s^2+20.5s+245}$$

The characteristic equation of the system is obtained by setting the denominator of the closed-loop transfer function to zero, we get

$$s^2+20.5s+245=0$$

$$s^2+2\zeta w_n s+w_n^2=0$$

we have

ζ =0.66 (damping ratio)

w_n=15 (natural undamped frequency)

$w_d=w_n\sqrt{1-\zeta^2}$ =11.1

$t_p=\pi/w_d$=0.2s (peak time)

M_p= 0.5 (maximum overshoot)

The unit-step response of the system is shown in Fig.3.B.2

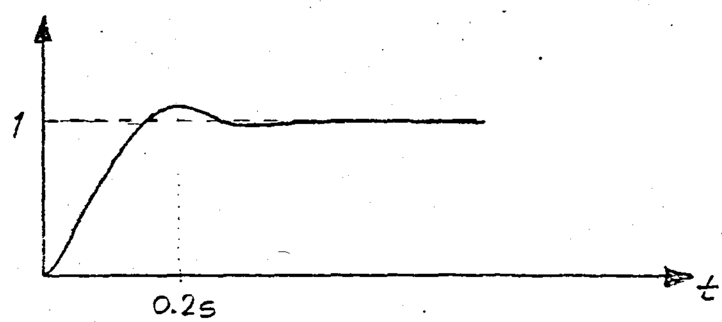

Fig.3.B.2 Unit-step response of the continuous-data motor control system.

Since the system is of the second order, the quadratic equation will always have roots in the left-half of the s-plane so long as all the parameters of the system are positive. Thus, the continuous-data system will always be asymptotically stable for all positive values of K_i, K_p, and K_m.

Now let us consider that the control system is subject to digital control. This is the practical case of our system.

The block diagram of the system is shown in Fig.3.B.3

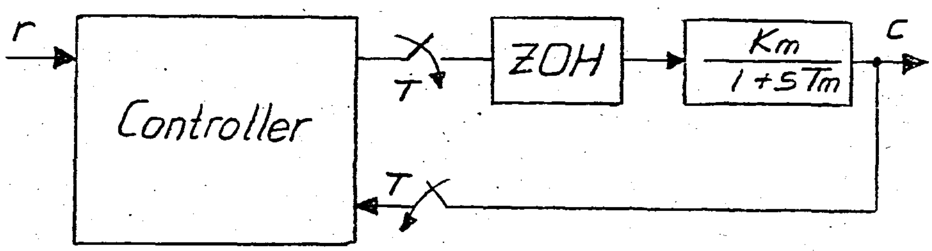

Fig.3.B.3 Block diagram of the digital control system

For the purpose of comparison we assume that the system parameters K_i, K_p are the same as those of the continuous data system. The pulse transfer function of the motor is written directly from Fig.3.B.3

$$G_M(z)=(1-z^{-1})Z\,\frac{K_m/T_m}{s(s+1/T_m)}$$

$$G_M(z)=\frac{K_m(1-\exp(-T/T_m))}{z-\exp(-T/T_m)}=\frac{B}{z-A}$$

Integral operation K_i/s can be approximated as

$$G_I(z) = \frac{K_i T(z+1)}{2(z-1)}$$

Therefore, complete block diagram is drawn as in Fig.3.B.4

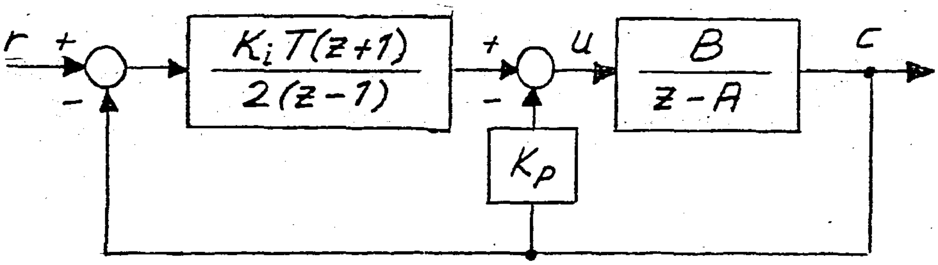

Fig.3.B.4 Digital IP control system.

The closed-loop transfer function of the system can be obtained as follows:

$$\frac{C(z)}{R(z)} = \frac{K_i TB(z+1)/2}{z^2+(-A+K_pB-1+K_iTB/2)z+A-K_pB+K_iTB/2}$$

Substituting the system parameters into the last equation, we have

$$\frac{C(z)}{R(z)} = \frac{0.403T(z+1)}{z^2+(-1.932361+0.403T)z+0.932361+0.403T}$$

The characteristic equation is obtained by equating the denominator of $C(z)/R(z)$ to zero

$$z^2+(-1.932361+0.403T)z+0.932361+0.403T=0$$

Since now there is an additional system parameter in the sampling period T, the performance of the overall digital control system will depend on the values of K_i, K_p, K_m, T_m and T.

Since the roots of the characteristic equation of the digital control system must stay inside the unit circle $|z|=1$ in the z-plane for the overall system to be asymptotically stable, we see that the second-order digital control system can be unstable for large values of T. Applying Jury's stability test to the characteristic equation:

z^0	z	z^2
0.932361+0.403T	-1.932361+0.403T	1

For stability

$$|a_0| < a_2$$

then

$$0 < T \leqslant 0.16635 \text{ sec.}$$

Therefore, for a stable operation, sampling period T must stay in this region.

Since the thyristor bridge must be controlled every 3.3ms, we must take the sampling period T as 3.3ms, and this is inside the stable region of T and sufficiently small.

For $K_i=120$, $K_p=9$, $K_m=0.94$, $T_m=0.46$ and $T=0.0033$sec, the closed-loop transfer function is

$$\frac{C(z)}{R(z)} = \frac{1.33\times10^{-3}(z+1)}{z^2-1.93z+0.93418}$$

The poles of the system are

$$z_{1,2}=0.965 \pm j0.05436$$

Absolute value of the pole is

$$|p_1| = 0.9665298$$
$$\phi_1 = \tan^{-1}(0.0543599/0.965)=3.224^{\circ}=0.056272 \text{ rad.}$$

By using the following equation we can find the damping ratio ζ,

$$|p_1| = \exp(-\zeta \phi_1/\sqrt{1-\zeta^2})$$

therefore

$$\zeta = 0.5176$$

The pole zero configuration of C(z)/R(z) is shown in Fig.3.B.5, from which we get

$$\alpha = -34.53^{\circ}$$

The maximum overshoot can be determined

$$M_p = 14\%$$

The peak time can be computed directly from the following eqation

$$T_{max} = \frac{T}{\phi_1}\left(\tan^{-1}\frac{-\zeta}{\sqrt{1-\zeta^2}} \mp \alpha + \pi\right)$$

$$T_{max} = \frac{0.0033}{3.224^{\circ}}\left(\tan^{-1}\frac{-0.5176}{\sqrt{1-(0.5176)^2}} + 34.53^{\circ} + 180\right)$$

$$T_{max} = 0.1879\,\text{sec}$$

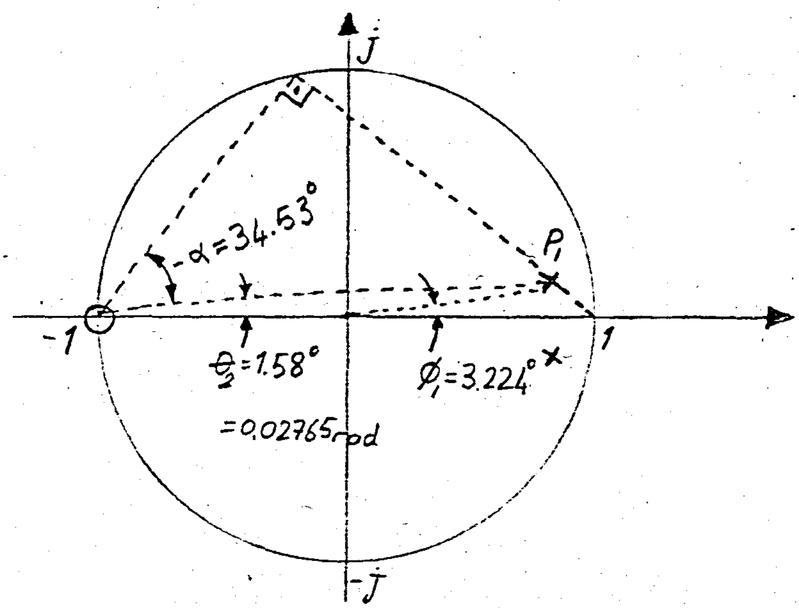

Fig.3.B.5 Pole zero configuration of the closed-loop transfer function, T=0.0033sec.

Step response of the digital system for T=3.3msec can be seen from Fig.3.B.6

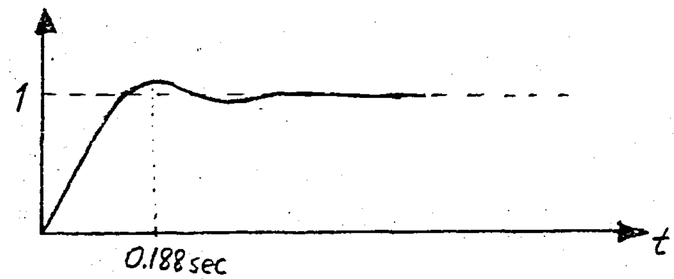

Fig.3.B.6 Step response of the digital system for T=3.3msec.

Since the sampling period is sufficiently small, the response of the digital system is approximately same as the continuous data system.

For T=1sec, it is expected that the digital system is unstable.

For the same parameters except the sampling period, $K_i=120$, $K_p=9$, $K_m=0.94$, $T_m=0.46$, and T=1sec, the characteristic equation is

$$z^2+56.3z+42.6$$

and

$$z_1=55.6$$

$$z_2=1.53$$

Since all the poles are outside the unit circle, the system is unstable.

Root locus diagram gives indication on the absolute and relative stability of a control system with respect to the variation of one system parameter K.

Since the characteristic equation of a linear time-invariant digital control system is a rational polynomial in z, the same set of rules devised for the construction of root loci in the s-plane can be applied to the z-plane.

– The open-loop transfer function of our system is

$$G_{OL}(z)= \frac{K_i TB(z+1)}{2(z-1)(z-A+K_p B)}$$

where $A=\exp(-T/T_m)$ and $B=K_m(1-A)$

If we take $K_p=9$, $K_m=0.94$, $T_m=0.46$, $T=0.0033$, and K_{ii} be the variable parameter, then the open-loop transfer function becomes

$$G_{OL}(z)= \frac{K_i 2.2179\mathrm{x}10^{-5}(z+1)}{2(z-1)(z-0.93)}$$

and the characteristic equation of the closed-loop system is

$$z^2+(-1.93285+K_i 0.00001108)z+0.99285+K_i 0.00001108=0$$

The root locus plot of the system when K_i varies between 0 and is constructed based on the pole zero configuration as shown in Fig.3.B.7. From the root locus we find that when the root locus cross the unit circle in the z-plane, the value of K_i is 11818.18. Thus, the critical value of K_i for stability is 11818.18.

Steady-state error of the system is zero since we introduced an integrator into the forward loop. It is easily seen that the steady-state error of the Integral-Proportional control system to a step input is zero, because the open-loop transfer function has a pole at z=1.

By choosing $K_i=120$ and $K_p=9$, we can obtain the desired response to a step input. But, we have made some simplifications while deriving the equations of the practical system. The terms that we have neglected can cause some problems. Therefore we must make a simulation and after some modifications on the values of parameters we can obtain the desired performance of the practical system.

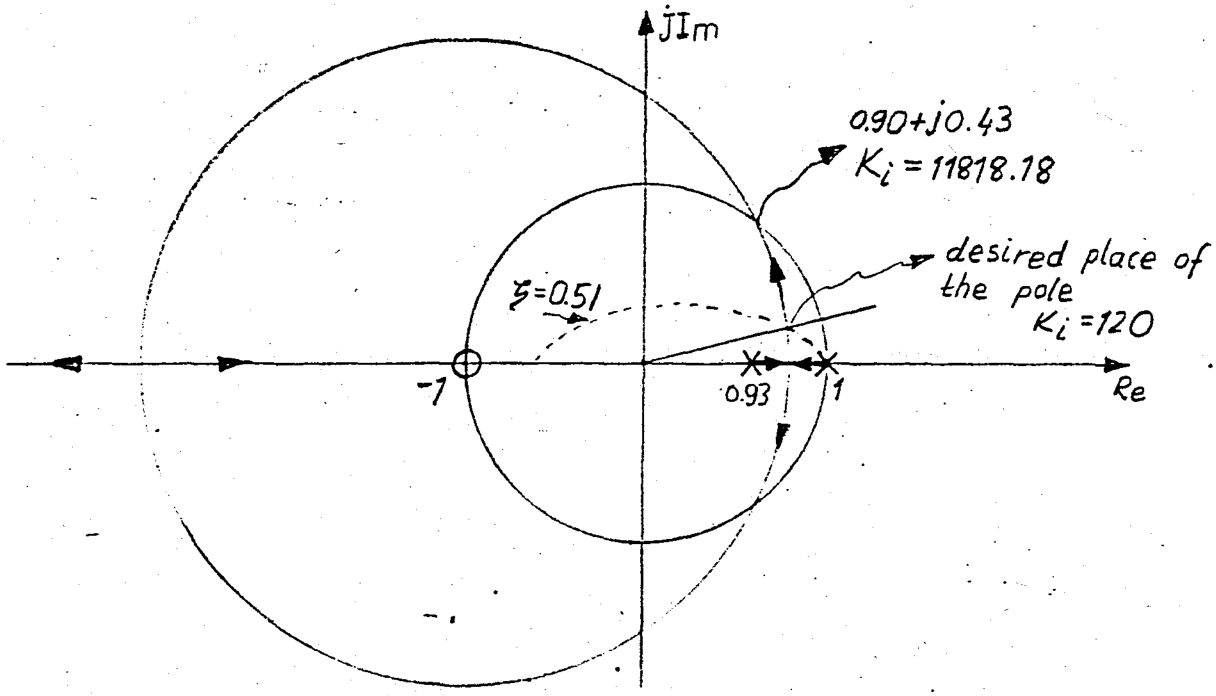

Fig.3.B.7 Root loci of the digital system.

For the simulation of the system, we will use the discrete state equations of the system. The continuous system, that is the motor that we control can be discretized as

$$x(k+1)=Ax(k)+Bu(k)$$

$$y(k)=x(k)=w(k)$$

where

$$A=\exp(-T/T_m)$$

$$B=K_m(1-A)$$

Also, we must obtain the discrete equation of the controller. Controller output u(kT) which corresponds to the armature voltage of the separately excited dc motor will be calculated from this equation for every sampling period.

Now, we can derive the necessary equations for the IP controller to obtain the desired control input to the dc motor. As you know, the purpose of the dc motor speed control system is to drive the load speed $w(t)$ to follow the constant command speed w_d. The error between the command speed and the load speed is

$$e(t)=w_d-w(t)$$

Thus, the input to the microprocessor is the digitized output speed signal $w(kT)$, $k=0,1,2,\ldots$. In the experimental set up, the output speed is obtained from the 10-bit A/D converter. The set speed w_d is saved in a memory location, and we let the output of the microprocessor be $u(kT)$.

The microprocessor is to perform the digital computation to implement IP controller so the continuous data form

$$u(t)=K_i\int e(t)dt-K_p w(t)$$

The integral in the last equation is written as

$$x(t)=\int_{t_o}^{t}(w_d-w(\tau))d\tau+x(t_o)$$

where t_o is the initial time, and $x(t_o)$ is the initial value of $x(t)$. To approximate the integral by a digital model several schemes may be used. We use the trapezoidal integration rule.

Let $t=kT$, $t_o=(k-1)T$, then the definite integral can be written as

$$x\ (t)=\int_{(k-1)T}^{kT}(w_d-w(t))dt+x((k-1)T)$$

The area between $(k-1)T$ and kT is approximated by a trapezoid

$$Area=e(k-1)T+(e(k)-e(k-1))T/2$$

then

$$x(kT)=Te((k-1)T)+T(e(kT)-e((k-1)T))/2+x((k-1)T)$$

However, in reality it takes the microprocessor a finite amount of time to compute the integral in this equation, so that given the input data $w((k-1)T)$ and $w(kT)$, the result of the integral computation is not available at $t=kT$. In general, we have to add up all the time intervals required to execute the OP-CODES of the integration subroutine on the microprocessor to find out what this time delay is. For convenience, we do all the computations in one sampling period T. This means that the right-hand side of the last equation gives the computational result of the integral at $t=(k+1)T$. Thus taking into account this time delay, integration result can be written as

$$x((k+1)T)=Te((k-1)T)+T(e(kT)-e((k-1)T))/2+x(kT).$$

Notice that we are using $x(kT)$ rather than $x((k-1)T)$ as the initial state of $x(t)$. Substituting $x((k+1)T)$ into the control equation, the discretizied version of the control word $u(t)$ can be written as

$$u((k+1)T)=K_i x((k+1)T)-K_p w(kT)$$

This control word is applied to the dc motor at $t=(k+1)T$ $k=0,1,2,...$

This control input is updated every T second, and is held constant between the sampling instants.

Now, we are ready to simulate the system in a digital computer. The equations that we must use are

$$w(k+1)=\exp(-T/T_m)\,w(k)+K_m(1-\exp(-T/T_m))u(k)$$

$$u(k+1)=K_i x(k+1)-K_p w(k)$$

In the simulation of the system, we took K_i and K_p as variable values because of the fact that we can easily change these values according to the requirements that we have chosen. Sampling period T is dependent on the control of the thyristor bridge. Since the bridge must be controlled every 1/6th interval of one period of the mains supply, it is constant and equal to 3.3msec. This sampling period is short enough for our system. It can cause no problem for the stability of the system.

The conversion of the output speed into a digital value by means of the A/D converter results in another block in the feedback. This should be taken into account. Since 1250rpm or 1250.2 /60 rad corresponds to 1024 bit, the gain of the A/D converter is 7.8bit/rad.

Simulation program and the results are shown at the appendix.

As seen, it is necessary to make a modification in the value of K_p in order to obtain the desired performance. A good response can be obtained for $K_p=3$.

C. Conclusion

As we have seen a digital system is an approximation of a continuous-data system. Besides the some parameters, sampling period is also an important factor that influences the respense of the overall digital system.

By choosing appropriate sampling period and placing the poles and zeros into the appropriate positions, we can obtain a good performance from the system. It is seen that for large parameters, we can obtain a fast response without overshoot(or very small overshoot) by means of the IP controller. As we have mentioned, the IP(Integral-Proportional) control system is different from the conventional PI control system.

We can make a comparison between the IP and the PI control systems. The pulse transfer function of the PI control system is as follows

$$G_{PI}(z) = \frac{Kz}{G_o(z)} + \frac{K'(z-1)}{G_o(z)}$$

where

$$G_o(z) = z^2 + (-A + K_p B - 1 + K_i TB/2)z + A - K_p B + K_i TB/2$$

By taking the same parameters for K_i and K_p chosen in the IP control, we simulate the PI control system. The output of this system is also shown in the appendix.

We can observe from these responses that the PI control system has larger overshoot than the IP control system. This overshoot is undesirable since it requires higher capacity of power converter. The reason of this overshoot is the extra term in the pulse transfer function of the PI control system. This term is eliminated in the IP control system, and response becomes fast and without overshoot. This term actually corresponds to the zero in the analog case. Therefore, we can say that the IP control system has better dynamic response than the PI control system.

During the operation of the system, motor may be effected by some disturbances like loading etc. In this case the system must recover the steady state value in a quickest manner. Therefore second point that we have to observe is the effect of loading. If we examine the block diagrams of both IP and PI control systems, the load-to-speed transfer functions of both system are the same. This transfer function is derived by assuming that the reference speed change is zero.

$$\frac{W_m}{V_\tau} = \frac{B(z-1)}{G_o(z)}$$

If the values of K_i and K_p are chosen large enough, the speed recovering time from a load change will be faster.

For the chosen values of the parameters, we can observe the change of speed from a load disturbance by means of the simulation.

From the simulation results, weconclude that using the IP control system we can obtain a fast response without overshoot, and also we can reduce the effects of the load disturbances. These can be achieved by choosing larger parameter values for K_i and K_p.

After obtaining the simulation results we can apply the designed parameters to the practical motor speed control system.

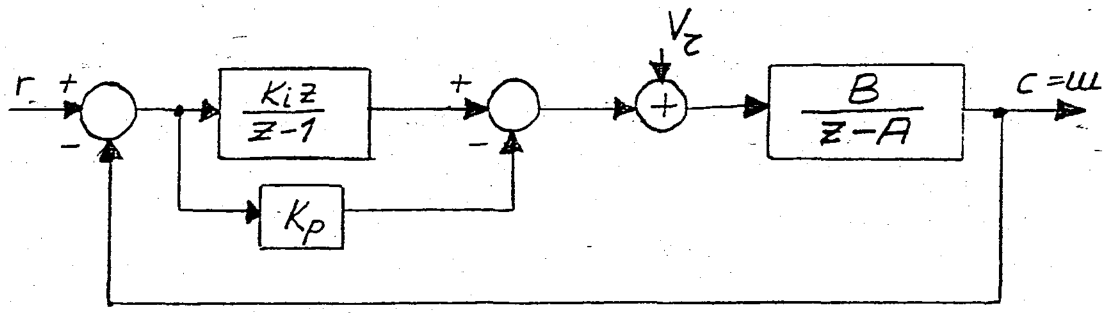

Fig.3.C.1 Simplified block diagram of PI control system.

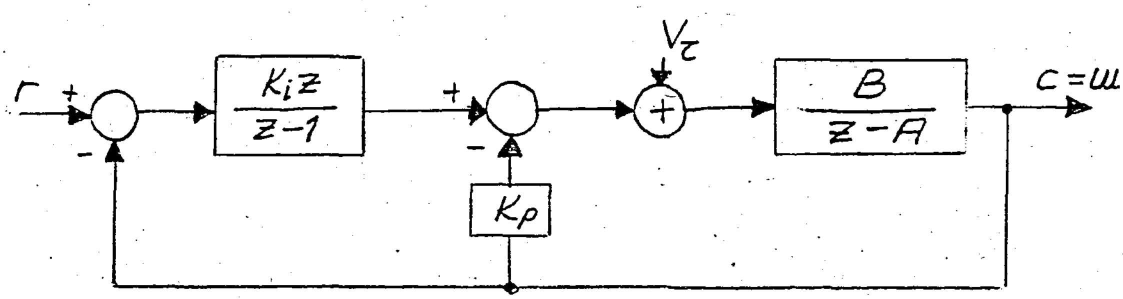

Fig.3.C.2 Simplified block diagram of IP contorl system.

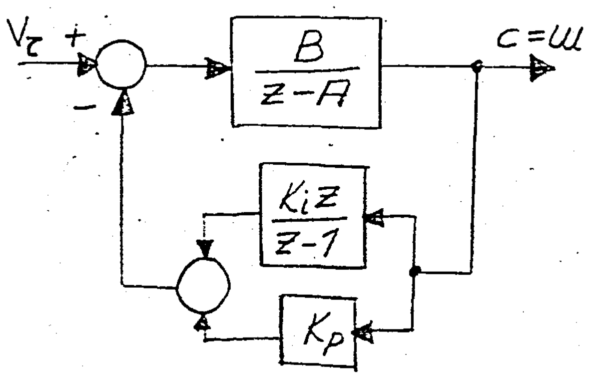

Fig.3.C.3 Load-to-speed block diagram of both PI and IP control systems.

TABLE 3.C.1 COMPARISON TABLE

IP		PI	
$\frac{W}{R}$	$\frac{K(z+1)}{G_o(z)}$	$\frac{K'z}{G_o(z)} + \frac{K''(z-1)}{G_o(z)}$	OVERALL TRANSFER FUNCTION
$\frac{W}{V_\tau}$	$\frac{B(z-1)}{G_o(z)}$	$\frac{B(z-1)}{G_o(z)}$	LOAD-TO-SPEED TRANSFER FUNCTION

Where

$$G_o(z)=z^2+(-A+K_pB-1+K_iTB/2)z+A-K_pB+K_iTB/2$$

IV. PRACTICAL SET UP

A. Introduction

In this chapter the design of a microprocessor based speed control of a dc motor fed by a three phase full-converter is described. The system is centered around a Z-80 based microcomputer with an external six bit counter, a PLL circuit, the synchronisation circuit, an ADC and the pulse amplifier. The firing angles are calculated by software, and IP control algorithm is introduced as controller.

B. Outline of the Practical System

A seperately excited dc motor with the ratings of 314 HP, 125V, 6A, and 1450rpm is being controlled by means of a three-phase full-converter, the output of which is directly controlled by a microcomputer.

In order to minimize the hardware, besides the control algorithm, the firing angles are also calculated by means of a microcomputer. The microcomputer used consists of Z-80uP which has a 2.5MHz clock and one input/output card. The system employs two eight-bit input ports and two eight-bit output ports

The interface between the microcomputer (or digital information) and the three-phase full-converter is performed by an external six bit counter which contains the required delay angle loaded from the output port (ØØ), a phase-locked-loop circuit which synchronizes the operation of the counter with the supply frequency, a current limiting circuit, and a

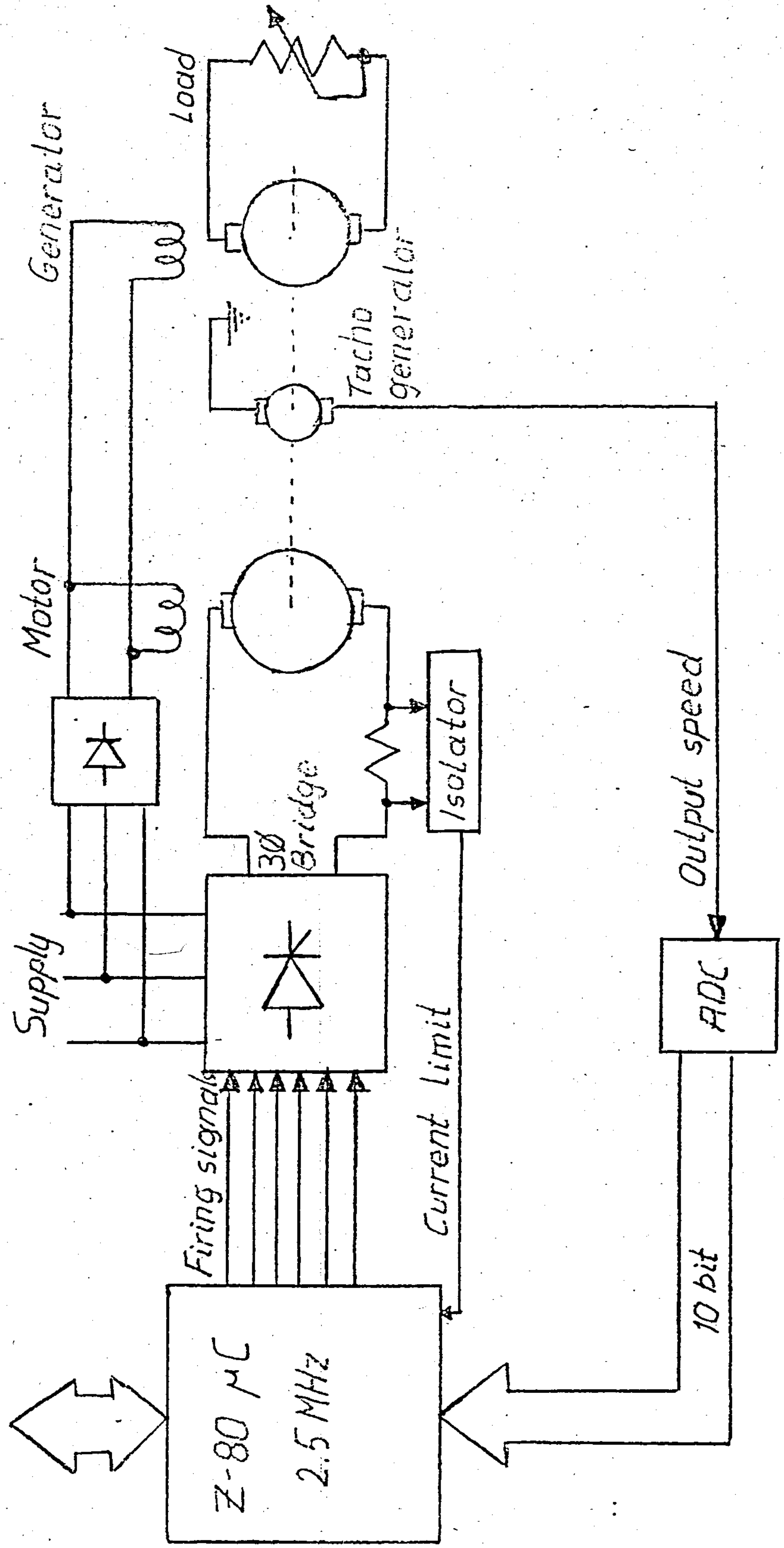

Fig.4.B.1 Block diagram of the complete system.

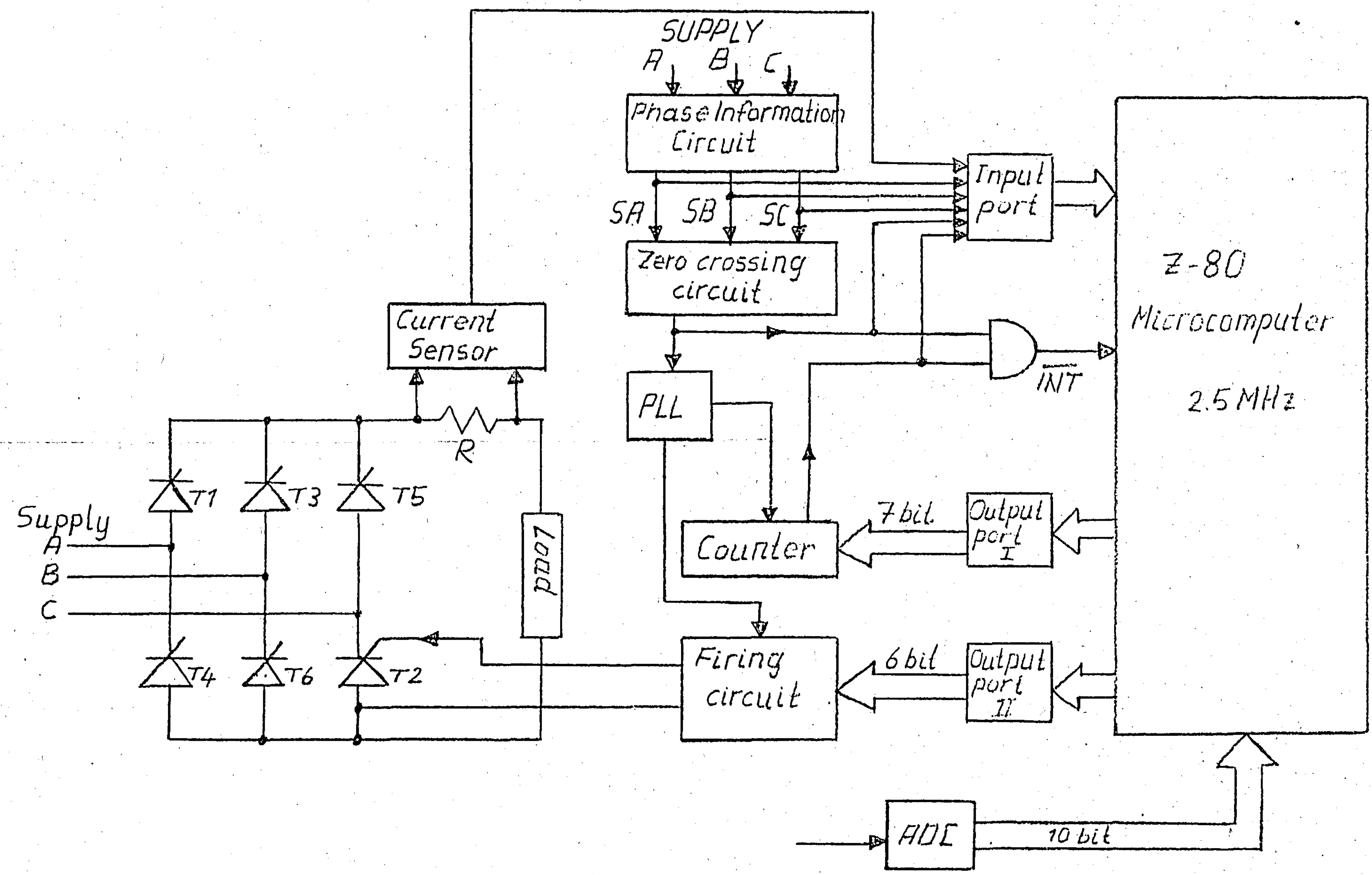

Fig.4.8.2 Detailed description of the blocks.

C. Three Phase Full-Converter

The output of the thyristor bridge (three phase full-converter) can be found as follows:
The supply voltages are

$$V_A=\sqrt{2}\ V\ \mathrm{Sin}\ wt$$

$$V_B=\sqrt{2}\ V\ \mathrm{Sin}(wt-2\pi/3)$$

$$V_C=\sqrt{2}\ V\ \mathrm{Sin}(wt+2\pi/3)$$

The output of the full-converter is

$$V_o(\alpha)=3/\pi\int_{\pi/6+\alpha}^{\pi/6+\alpha+\pi/3}(V_A-V_B)d(wt)$$

therefore

$$V_o(\alpha)=\frac{3\sqrt{6}}{\pi}\ V\ \mathrm{Cos}\alpha$$

$$V_o(\alpha)=1.35\ V_{LL}\mathrm{Cos}\alpha \qquad (4.C.1)$$

where V_{LL} is the rms value of the line to line voltage.
The thyristor converter characteristic is shown in Figure 4.C.1
This is a cosine curve, and the gain of the thyristor amplifier changes considerably with the firing angle.

The gain of the thyristor amplifier is given by $dV_o/d\alpha$, and

$$dV_o/d\alpha=-1.35\ V_{LL}\ \mathrm{Sin}\ \alpha \qquad (4.C.2)$$

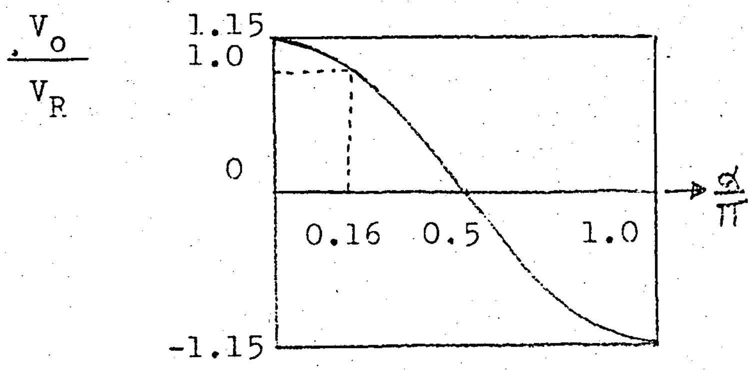

Fig.4.C.1 Thyristor bridge characteristic .

The relation between the control word, u, and the firing angle, α, is also nonlinear. In order to obtain a good rosponse, a linear relation between the control word, u, and the bridge output, V_o, must be obtained. This linearization operation can be done as follows:

$$\alpha = \text{Cos}^{-1}(Ku)$$

and

$$V_o = 1.35\ V_{LL}\ \text{Cos}\,\alpha$$

substituting α into V_o, we obtain

$$V_o = 1.35\ V_{LL}\ \text{Cos}(\text{Cos}^{-1}(Ku))$$

$$V_o = 1.35\ V_{LL}\ Ku$$

$$= K_c u \qquad (4.C.3)$$

In the software, the pozitive values of u are limited to

+96dec. For calculated values of the control word, corresponding firing angles are calculated by the Eq.(4.C.4) , and these values are multiplied by 64/60 for the inverse of the counter resolution.

$$\alpha_{deg} = \mathrm{Cos}^{-1} |u| /96 \qquad (4.C.4)$$

According to these values, an inverse cosine look up table is constructed, and the required delay angles which are loaded into the external counter at the instants when a zero crossing interrupt occurs are stored into the memory at the beginning of the program execution. Hexadecimal values of the firing angles are listed in the FIRING ANGLE LOOK UP TABLE.

The gain of the converter can now be easily obtained by the following equation,

$$V_o = 1.35\ \mathrm{Cos}(\mathrm{Cos}^{-1} |u|/96)\ V_{LL}$$

$$= 1.35\ \frac{100}{96} |u|$$

$$V_o = K_c |u|$$

Therefore, the gain of the bridge,

$$K_c = V_o / |u| = 1.4 \qquad (4.C.5)$$

Figure.4.C.2 shows the bridge output voltage as a function of the control word. Because of the experimental difficulties, the whole range of the regeneration mode could not be tested. The dotted lines show the theoretically expected values.

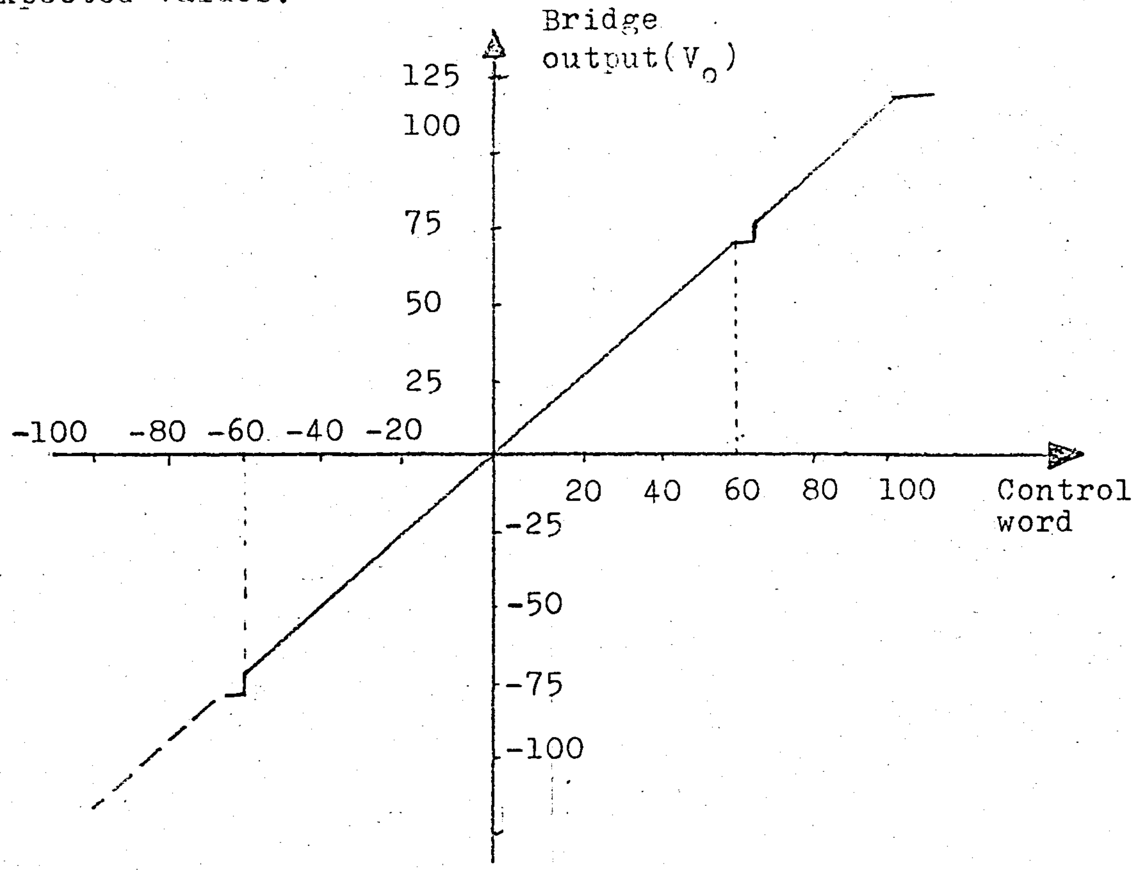

Fig.4.C.2 Bridge input/output characteristics.

It is seen from Figure. 4.C.2 that the control is smooth and linear except for the values of the control word corresponding to the firing angles around 60^{o} and 120^{o}. This is because of the limitations over the count values. These limitations will be discussed later in the software.

FIRING ANGLE LOOK-UP TABLE

5F	5F	5F	5E	5D	5D	5C	5C	5B	5A	5A	59
58	58	57	56	56	55	54	54	53	53	52	51
51	51	4F	4F	4E	4D	4D	4C	4B	4B	4A	49
49	48	48	46	46	45	44	44	43	42	42	3A
3A	3A	3A	3A	3A	3A	3A	3A	39	38	38	37
36	35	34	33	33	32	31	31	2F	2E	2D	2C
2B	2A	29	28	27	26	25	24	23	21	1F	1F
1E	1C	1B	19	17	16	14	12	ØF	ØC	Ø8	Ø2
Ø2											

V. THE SOFTWARE

A. Firing Angle Control

As mentioned earlier, the firing angles corresponding the calculated control words are obtained by a software method. In chapter IV the practical system was briefly described Here we will look the system more detailed since some terms like range, three phase information etc. will then become more clear.

Firing signals are sent to a chosen pair of SCR gates at the same time for both continuous and discontinuous current modes as shown in Fig.5.A.1. Once each firing gate pulse is generated, it is held active for 60°, and in order to fire the SCRs reliably, these pulses are ANDED with a frequency of 19.2kHz obtained from the PLL. The advantage of this method is that it gives us more time to calculate the control algorithm since generation of the short firing pulse train during that interval will take a lot of time when we attempt it to generate by software method.

The firing angle command corresponding to the control word is stored in a look-up table. This contains 8-bit absolute data, D7-DO. D7 and D6 indicate one of the ranges of 0°-59°, 60°-119°, 120°-179°. D5-DO represent the angle from 0° to 59°. During the one-sixth period of ac source, there are three sources to be controlled. For example, if the digitized power signals are SA=1, SB=0, and SC=Ø, the wave forms of the power sources are shown in Fig.5.A.2. In this case, the power sources

Vab, Vcb and Vca, are used to control the positive current. Vab will be chosen as the power source in case the firing angle is in the range of 0°-59°, and Vcb will be chosen if the range is 60°-119°, and Vca will be chosen if the range is 120°-179°. By this algorithm, the full range of 0°-179° can be controlled within one-sixth period of ac source. Thus the design of overall system compensation is simplified and the overall response is increased.

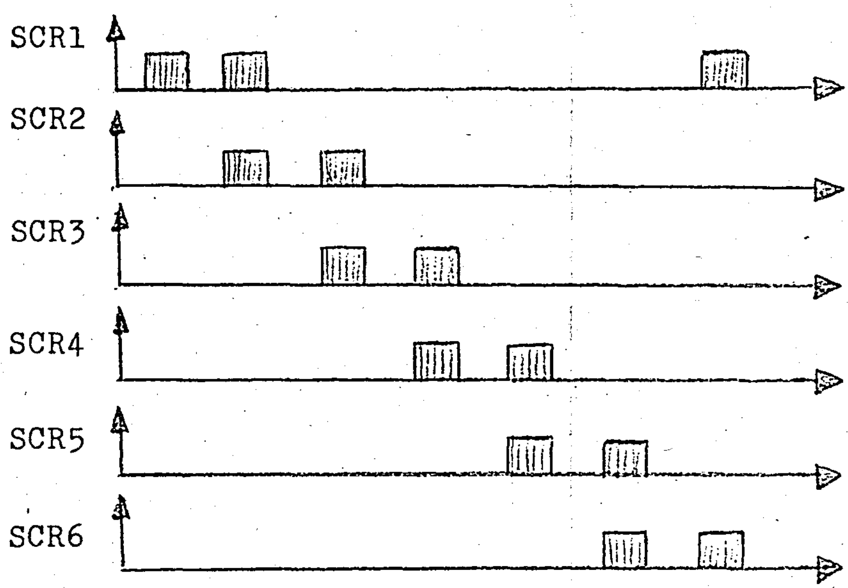

Fig.5.A.1 SCR gate signals.

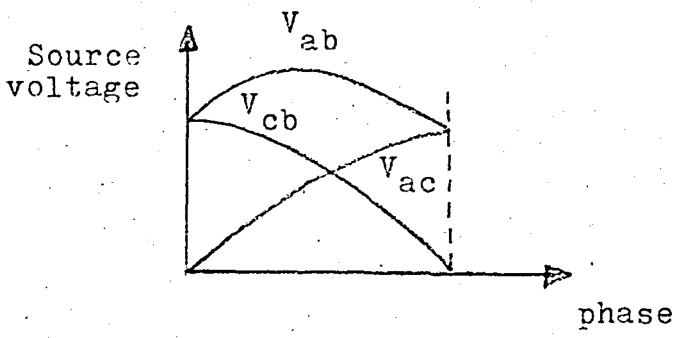

Figure 5.A.2 Power source voltage signals.

The firing range selection is implemented by table look-up algorithm as shown in Table 5.A.1. The software program for the firing control is described in the next section.

TABLE 5.A.1 Truth table for firing control

INPUT					OUTPUT							
D7	D6	SA	SB	SC	1	2	3	4	5	6	SOURCE	ANGLE
0	0	1	0	1	0	0	0	0	1	1	Vcb	
0	0	1	0	0	0	0	0	0	0	1	Vab	
0	0	1	1	0	1	1	0	0	0	0	Vac	0^o-60^o
0	0	0	1	0	0	1	1	0	0	0	Vbc	
0	0	0	1	1	0	0	1	1	0	0	Vba	
0	0	0	0	1	0	0	0	1	1	0	Vca	
0	1	1	0	1	0	0	0	1	1	0	Vca	
0	1	1	0	0	0	0	0	0	1	1	Vcb	
0	1	1	1	0	1	0	0	0	0	1	Vab	60^o-120^o
0	1	0	1	0	1	1	0	0	0	0	Vac	
0	1	0	1	1	0	1	1	0	0	0	Vbc	
0	1	0	0	1	0	0	1	1	0	0	Vba	
1	0	1	0	1	0	0	1	1	0	0	Vba	
1	0	1	0	0	0	0	0	1	1	0	Vca	
1	0	1	1	0	0	0	0	0	1	1	Vcb	120^o-180^o
1	0	0	1	0	1	0	0	0	0	1	Vab	
1	0	0	1	1	1	1	0	0	0	0	Vac	
1	0	0	0	1	0	1	1	0	0	0	Vbc	

B. Software Algorithm of IP Controller

In the development of the software the following points are taken into consideration.

(A) The software program must be written such that it will be applicable to the closed-loop systems, in other words, both firing algorithm and the program that calculates the control word must be written in one sampling period. This says that the control word calculated in this sampling period is used for controlling the bridge, in the next period. Since the sampling period is 3.3ms, therefore, a control delay of one period is unavoidable.

(B) Precaution is taken to ensure that all the interrupts receive servicing properly.

(C) The relation between the output voltage of the three-phase six-pulse bridge and the firing angle is a cosine curve. In order to obtain a linear relation for the control word, u , and bridge output an inverse cosine look up table should be stored in the memory.

(D) It must be possible to change the integral and proportional parameters, and increase or decrease the motor speed.

Z-80 microprocessor can operate in three different interrupt modes. In this case, the most suitable one is the fir mode. In this mode, there is no need for an external hardware to load the counter with an interrupt vector, and an interrupt signal cause the program to return to ØØ38H address.

General flow chart of the program is shown in Figure When an interrupt is sensed, the instruction in ØØ38H which determines the starting place of the program is loaded into the program counter. There are two interrupt sources, one is the zero crossing pulse, the other is the count zero pulse which is produced when the external six bit programmable counter counts down to zero. First interrupt pulse goes to the microcomputer from the LSB of the input port Ø1 of the I/O card, latter goes from the 2nd SB of the input port Ø1. These two pulses are negative ORED in the external interface circuit and output of which is applied to the interrupt pin of the Z-80 microprocessor. Since these are two interrupt sources, first work to be done is to examine which source caused the interrupt. If this is due to the zero crossing pulse, the count valve calculated in the previous period is loaded into the external counter, counter is enabled and the triggering pulses applied in the last period are cleared. Interrupt is enabled (EI) and the main program is entered. Main program includes the necessary control algorithm. In this program, control word is calculated, an inverse cosine table is consulted Six LSBs are used as count valve corresponding to the delay angle at the next cycle. The two MSBs are stored in order to be used in the determination of the range of the delay angle, i.e between 0°-60°, or 60°-120°, or 120°-150°. The microcomputer then goes to the HALT state.

When the counter which is loaded with the previous count value counts down to zero, the count zero interrupt pulse is produced and this interrupt causes the program to branch into the firing routine. Upon entering the firing routine, the registers are saved because the count zero interrupt signal may come in any point of the branch of the program and registers, therefore, must be saved to be used afterwards.

Then, by checking the status of the armature current (6thSB of the input port Ø1), it is tested whether the load current is above or below the maximum value of the current. It is normally high, but goes to the low whenever an overcurrent occurs. In the case of overcurrent, no SCRs are fired and returned to the main program.

If the current has not reached to the maximum value, a new phase information, i.e. SA,SB and SC are taken. The two bit (D_7 and D_6) range information, stored in the previous cycle and SA, SB, and SC together determine the SCR which must be triggered. The look-up table used for this purpose is shown in the Table

During the firing routine, the microprocessor is disabled against to the interrupts, therefore, execution time must be as short as possible. If a software approach is used to produce the firing pulses, pulse duration which should be at least 100-150μs increases the execution time. One way to overcome this problem is to allow the pulses to be held at the gates until the next period. As the I/O card used has latch circuit, the use of this method has become possible.
After reloading the registers with their previous values, the interrupt flip-flop is enabled. A return from interrupt instruction causes the program to go back either to the main program or HALT state.

The flow chart of the main program is shown in Figure 5.E.2. Although only the absolute numbers are used, it is possible to apply the sign bit arithmetic. We applied both arithmetic and saw that the execution times of both method are approximately the same, but writing the assembly language (at the point of view of ease) of the program using sign bit arithmetic is shorter than the other.

Since the error is calculated at the beginning of the main program, a reference speed is stored in a memory location. Actual motor speed is sensed with a tachogenerator, output of which (dividing to a suitable level) goes to the ADC which is a DATEL ADC-856 ten bit converter. 8 most significant bits of the A/D converter go to the input port ØØ, but the two least significant bits go to the most significant bits of the the input port Ø1. That is, we obtain an output speed which consists of ten bits. This binary value is stored as INSPD in the memory, since it is also used later in the program. After the error is found, it is added to the previous value of the error. This sum is called BETA, that is, $B= e(k)+e(k-1)$. Then BETA is added to the old integral value, and as a result the integrator output is obtained, ie, $x(k)$. Note that, we assumed that the coefficient, $K_I T/2$ of the integrator is equal to 1, therefore $K_I=66$. In order to simplify the program further, we assumed $16K_I T/2$ is equal to one. From here K_I is equal to 37.8 or approximately equal to 40.

In the same way, we assumed that motor speed coming into the proportional controller is equal to 16 times the speed i.e $16w(k)$. After multiplying by K_p , and substracting from $16K_I T/2.X(k)$ we obtain the following control word:

$$16\,u(k+1) = \frac{16K_iT}{2}\,x(k) - 16K_p w(k)$$

Next step is to divide $16\,u(k+1)$ by 16 to obtain the actual control word. Then corresponding count value (delay angle) is extracted from the look-up table.

Here a remark must be made. When the control words take negative values, we don't consult to the look-up table. In this case, we follow another approach which is based on mathematical calculations:

The characteristics of the bridge is approximately as follows (Figure 5.B.3)

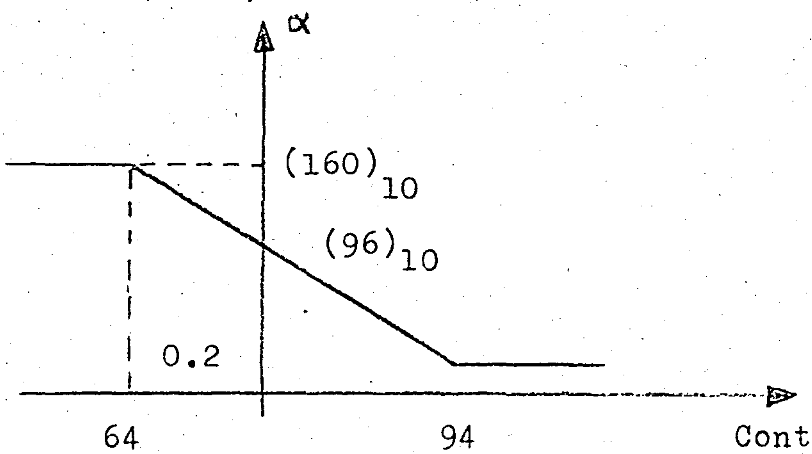

Fig.5.B.3 characteristics of the bridge

As it is seen that maximum negative control word, U_k, is equal to 64 so that $\alpha < (160)_D$. After the calculation of the control word, we remember to limit α to 02^{o}-57^{o}.

If the control word is negative, as you see from the characteristic that we must add $96_{dec.}$ to the negative U_k such that the corresponding delay angle, α, is found.

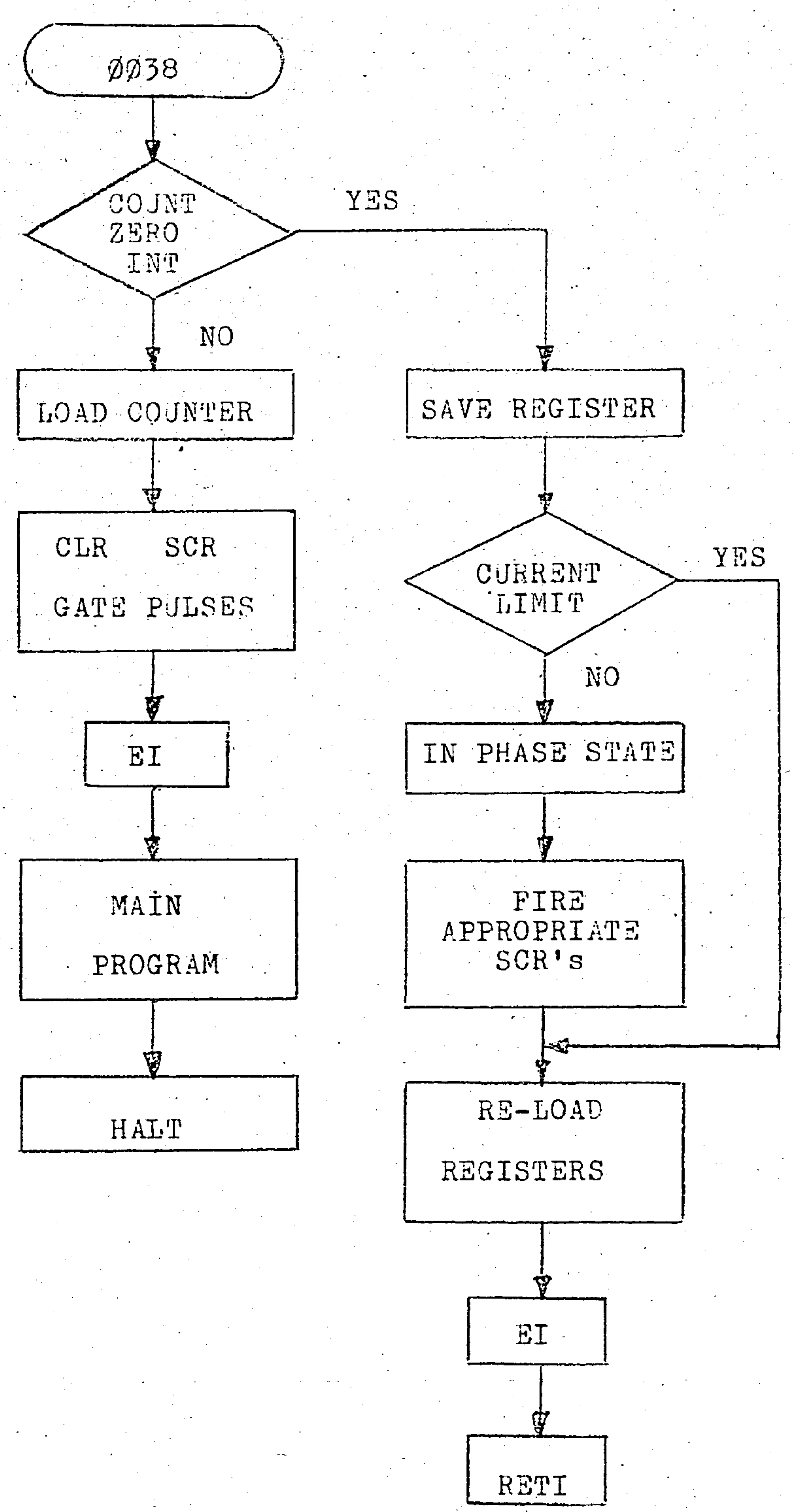

Fig.5.B.1 General flow chart.

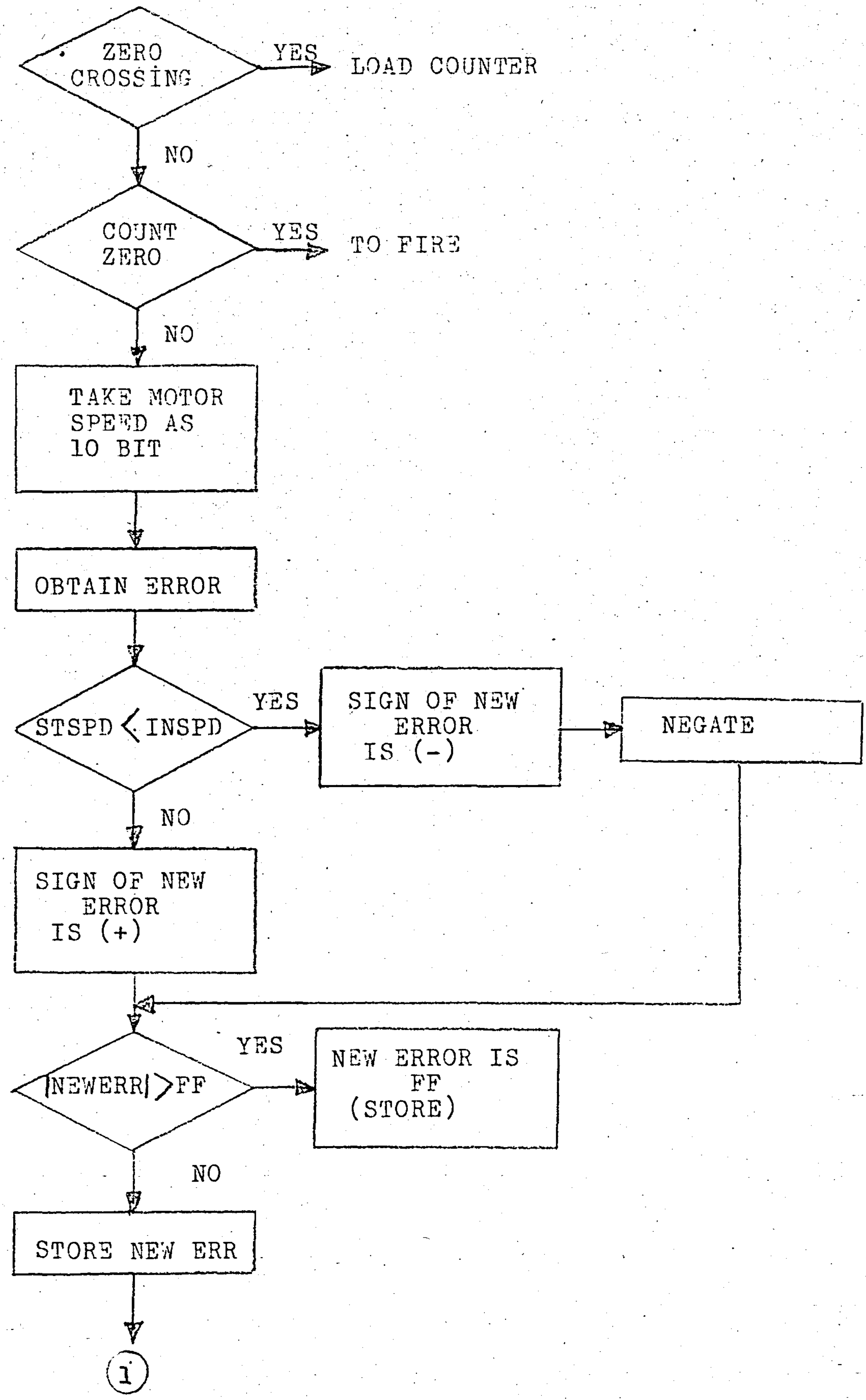

Fig.5.B.2 Flow chart of the Main program.

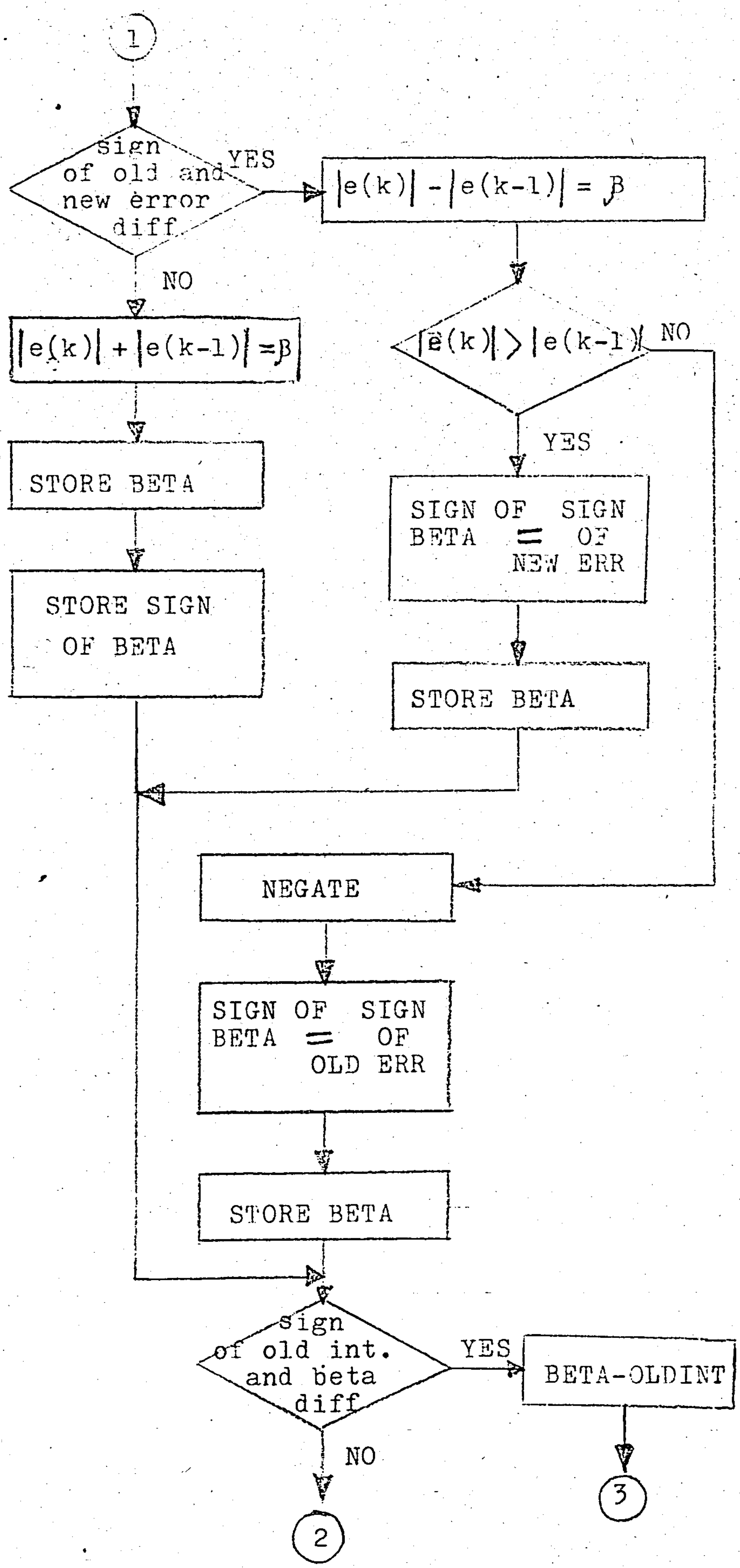
1
sign of old and new error diff
YES
$|e(k)| - |e(k-1)| = \beta$
NO
$|e(k)| + |e(k-1)| = \beta$
$|e(k)| > |e(k-1)|$
NO
YES
STORE BETA
SIGN OF BETA = SIGN OF NEW ERR
STORE SIGN OF BETA
STORE BETA
NEGATE
SIGN OF BETA = SIGN OF OLD ERR
STORE BETA
sign of old int. and beta diff
YES
BETA-OLDINT
NO
3
2

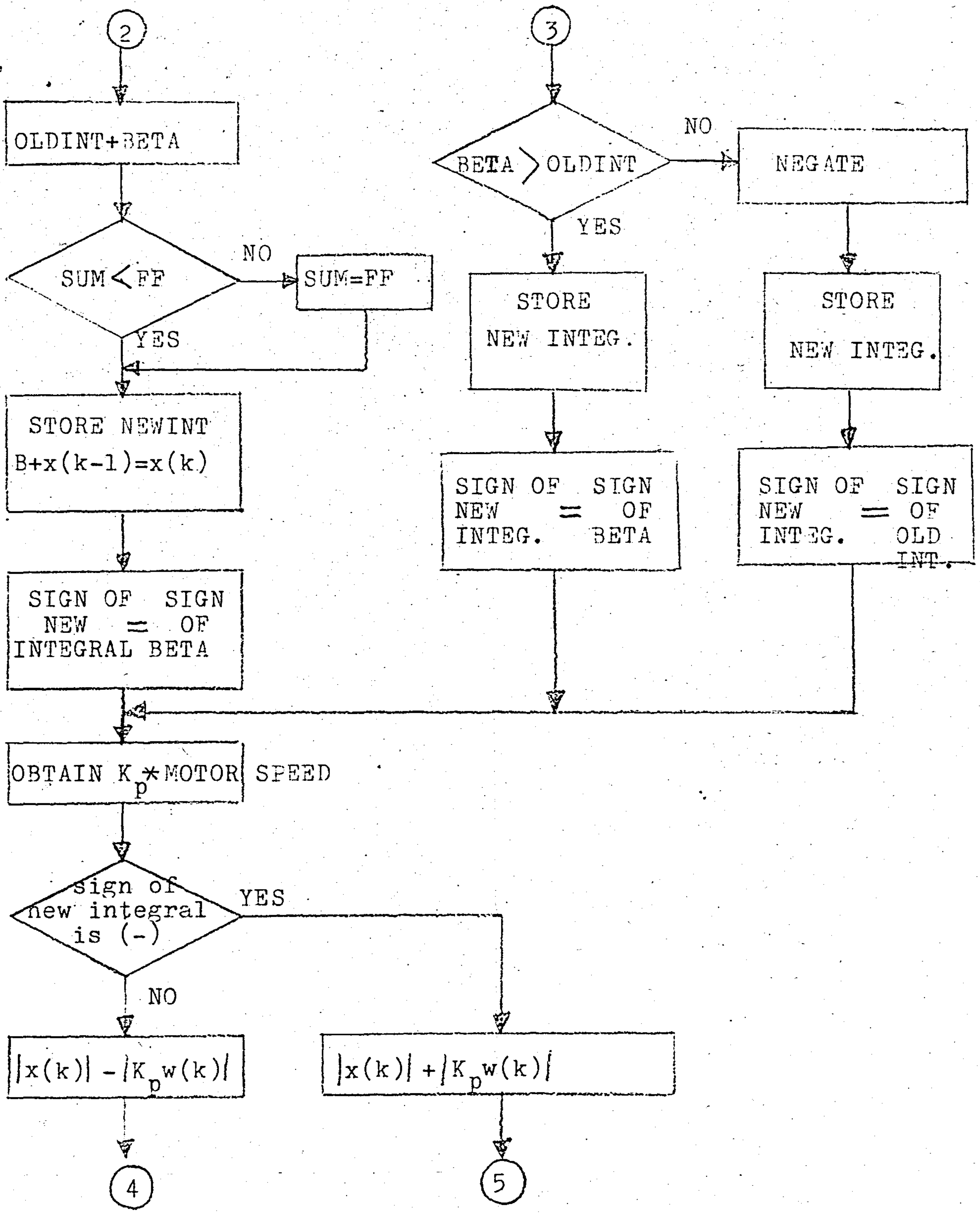
2
OLDINT+BETA
SUM < FF
NO
SUM=FF
YES
STORE NEWINT
B+x(k-1)=x(k)
SIGN OF NEW INTEGRAL = SIGN OF BETA
3
BETA > OLDINT
NO
NEGATE
YES
STORE NEW INTEG.
STORE NEW INTEG.
SIGN OF NEW INTEG. = SIGN OF BETA
SIGN OF NEW INTEG. = SIGN OF OLD INT.
OBTAIN K p * MOTOR SPEED
sign of new integral is (-)
YES
NO
|x(k)| - |K p w(k)|
|x(k)| + |K p w(k)|
4
5

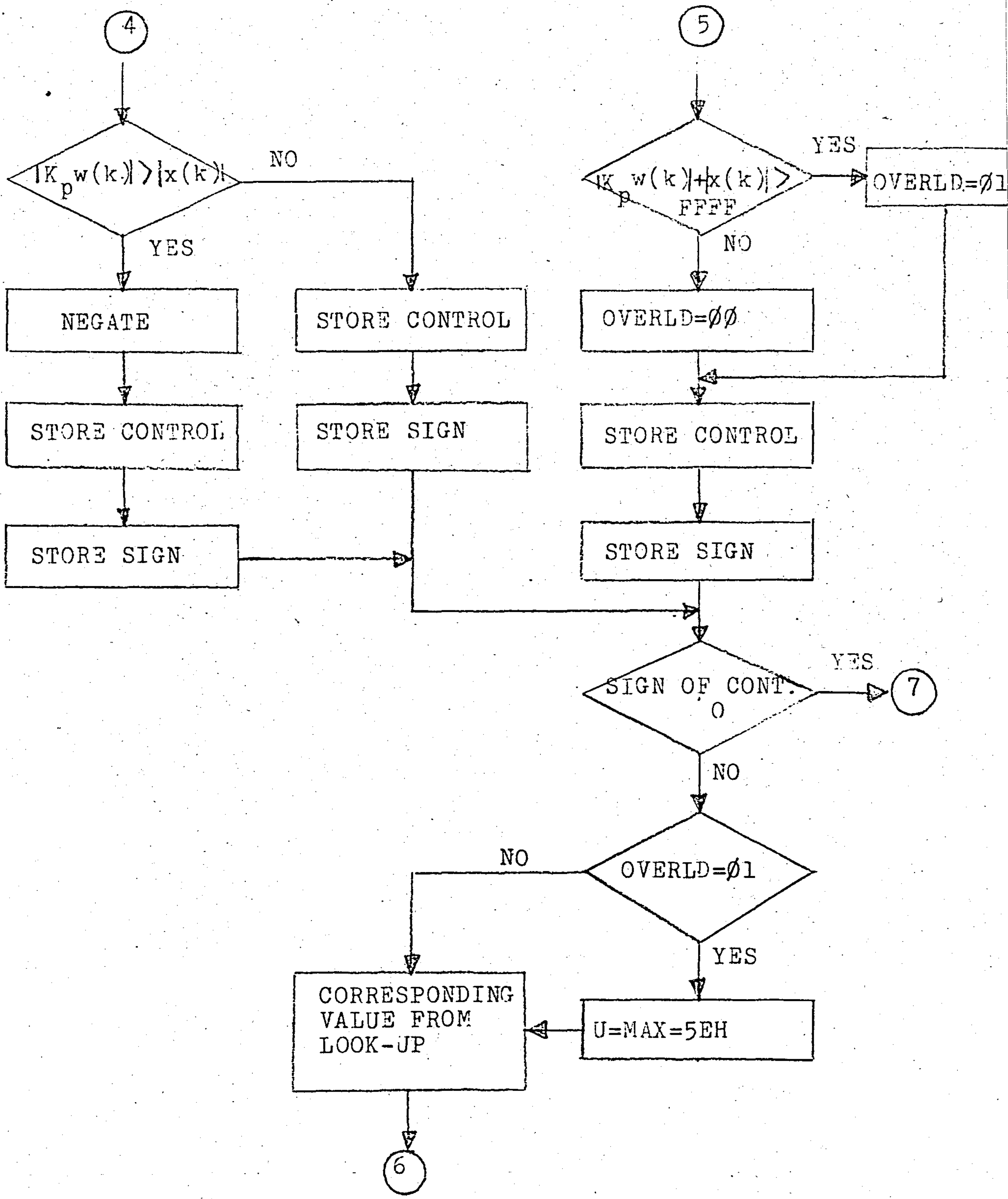
4
5
|Kpw(k)| > |x(k)|
NO
YES
NEGATE
STORE CONTROL
STORE SIGN
STORE CONTROL
STORE SIGN
|Kpw(k)|+|x(k)| > FFFF
YES
OVERLD=Ø1
NO
OVERLD=ØØ
STORE CONTROL
STORE SIGN
SIGN OF CONT. 0
YES
7
NO
OVERLD=Ø1
NO
YES
U=MAX=5EH
CORRESPONDING VALUE FROM LOOK-UP
6

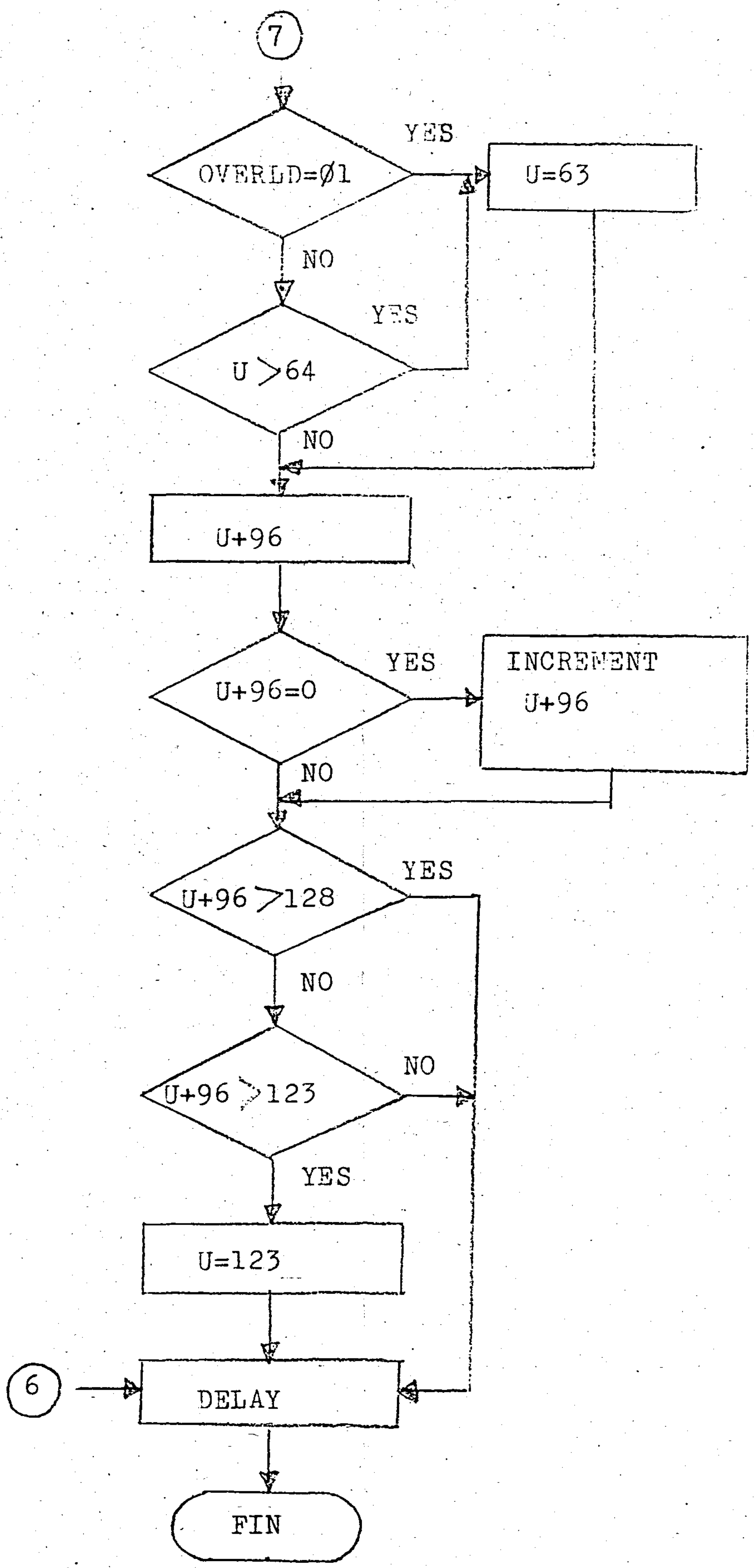
7
OVERLD=Ø1
YES
U=63
NO
YES
U >64
NO
U+96
U+96=0
YES
INCREMENT
U+96
NO
U+96 >128
YES
NO
U+96 >123
NO
YES
U=123
6
DELAY
FIN

C. Limitations in the Software

1. Interrupt Pulse Width:

There are two interrupt sources. When an interrupt Occurs, the microcomputer must understand where it comes. During which a time interval passes. Therefore, the width of the interrupt pulse should be adjusted according to this. However, this width must be such that both interrupts cannot occur at the same time. Due to the above limitations, monostables producing these interrupt pulses are adjusted to a pulse width of 40μs.

2. Limitations on the Count Value:

Theoretically, the bridge can be operated by a firing angle which extends between 0^{o} and 180^{o}. However, in practice, for a reliable operation, some limitations should be made at both ends of this range. These limitations are known as "forward and backward" limitations or "terminal stops". Therefore, the range of the count value is limited to 1-160. These values correspond to the firing delay angle range of approximately 1^{o}-150^{o}.

After a zero crossing interrupt signal has come the interrupts are disabled until the interrupt reason is understood. Therefore, in order to ensure that the software operates correctly, the count value of the counter should not cover all the range of 0-64. The limits are experimentally determined and limited to 1-60.

VI. CONCLUSION

The microprocessor-based digital speed control system of motor drive is discussed and a new control algorithm (IP) which is superior than the conventional PI control system have been achieved.

The system suffers from two serious problems; one is the time lag problem, which inherently exists in a digital control system, the second is the data detection delay time.

Output speed is measured with a tracking type A/D converter which detects the instantaneous speed at lower speeds, and it is assumed that the data detection delay problem is overcomed for a large amount.

A microprocessor-based digital control system inherently contains a control lag for processing the control signal. The execution time for processing the control program of the system is not so short as compared with a sampling period. Therefore, this control lag also affects the response and the stability of the system.

A predictive state observer can be introduced to solve the two above mentioned problems. The predictive state observer gives the estimated values of the instantaneous speed on the next sampling instance before the actual time is reached. This operation of the predictive state observer compensates both the detection lag and the control lag. But introduction of the state observer into the system results in more multiplication operations of the computer than the original IP control algorithm.

This requires a hardware multiplier.

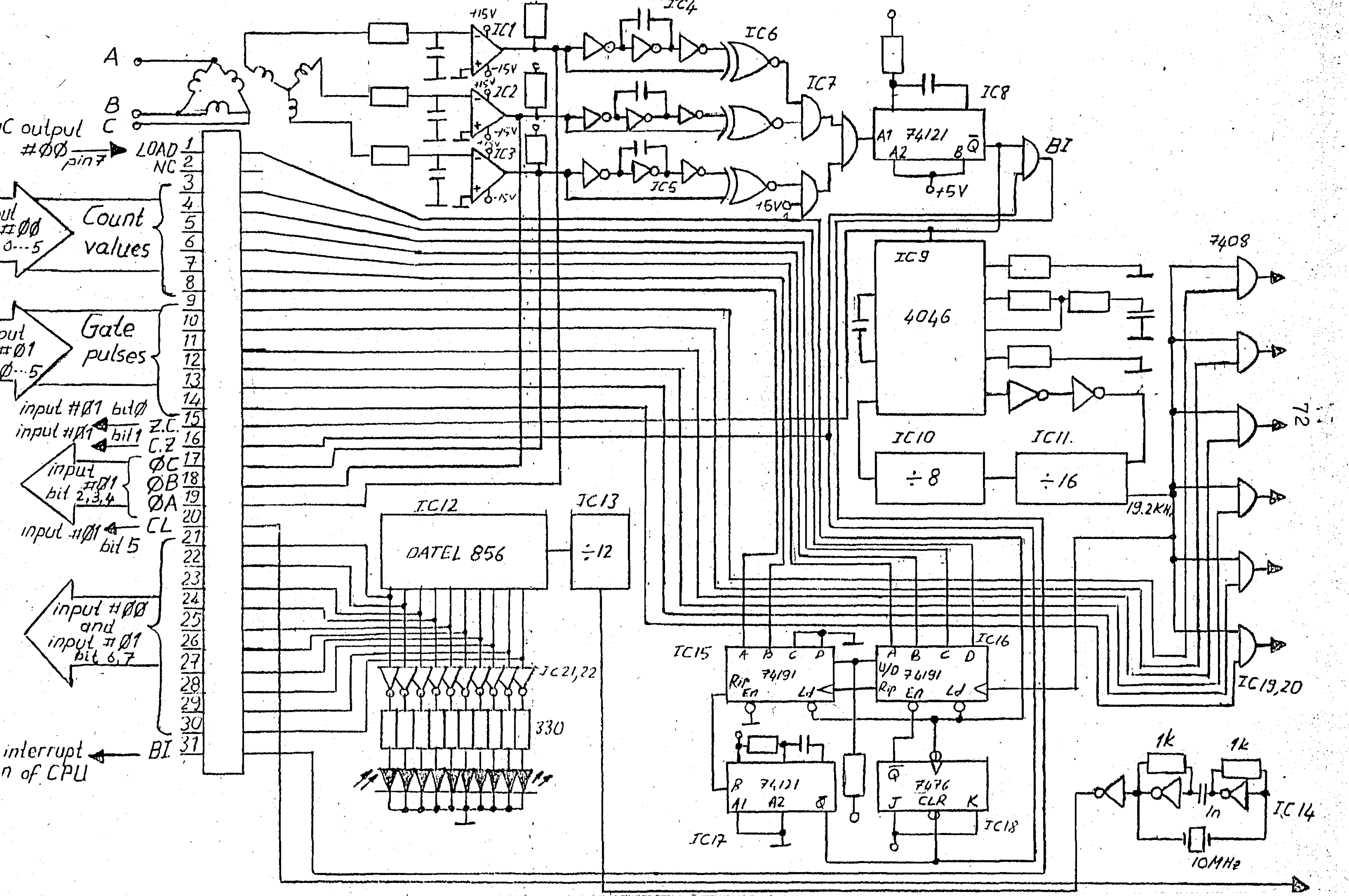
A
B
C
C output
#ØØ pin7
LOAD
NC
Count values
Gate pulses
input #Ø1 bitØ
input #Ø1 bit1
Z.C.
C.Z
input #Ø1 bit 2,3,4
ØC
ØB
ØA
input #Ø1 bit 5
CL
input #ØØ and input #Ø1 bit 6,7
interrupt
of CPU
BI
IC1
IC2
IC3
+15V
-15V
IC4
IC5
IC6
IC7
IC8
A1
74121
A2
+5V
IC9
4046
IC10
÷8
IC11
÷16
19.2KH
7408
IC19,20
72
IC12
DATEL 856
IC13
÷12
IC21,22
330
IC15
74191
IC16
U/D
Rip
En
Ld
IC17
IC18
7476
CLR
1k
IC14
10MHz

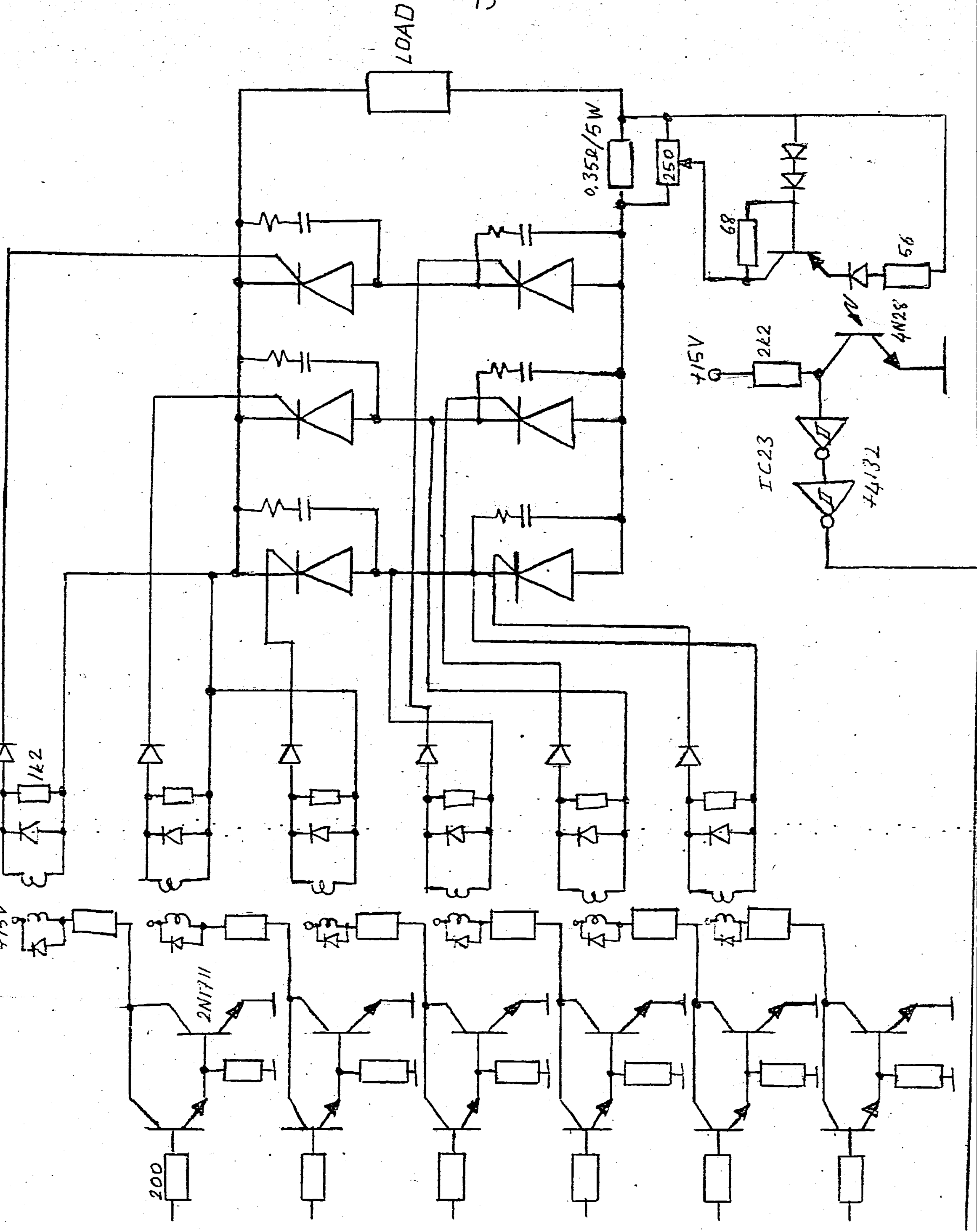

LOAD
0,35Ω/5W
250
68
56
4N28
+15V
2k2
IC23
74132
1k2
2N1711
200

APPENDIX A

SIMULATION RESULTS

From discrete state equation of both controller and motor, we can easily simulate the system in a digital computer. The simulation program written in BASIC is as follows:

```
...SPEED RESPONSE...
10 KI=... :KP=... :KM=.94:TM=.46
20 T=0.0033:K=0
30 A=EXP(-T/TM):B=KM*(1-A)
40 R=10:EK=0:EK1=0:X=0
50 EK=R-Y
60 X=T*(EK+EK1)/2+X
70 U=KI*X-KP*Y
80 W=A*W+B U
90 Y=7.8*W
100 K=K+1
110 PRINTK,Y
120 EK1=EK
130 GOTO 50
140 STOP
```

For the PI control system, only the control word is different:

```
70 U=KI*X+KP*EK
```

Load-to-speed block diagram of both system is the same. Simulation program is shown below,

```
...LOAD CHANGE...
10 KI=... :KP=... :KM=0.94:TM=0.46
20 T=0.0033:K=0:X=0
30 A=EXP(-T/TM):B=KM*(1-A)
40 W=0:VT=1
60 X=T*W*7.8+X
70 U=KI*X+KP*W*7.8
80 E=VT-U
90 W=A*W+B*E
100 K=K+1
110 PRINTK,W
120 GOTO 60
130 STOP
```

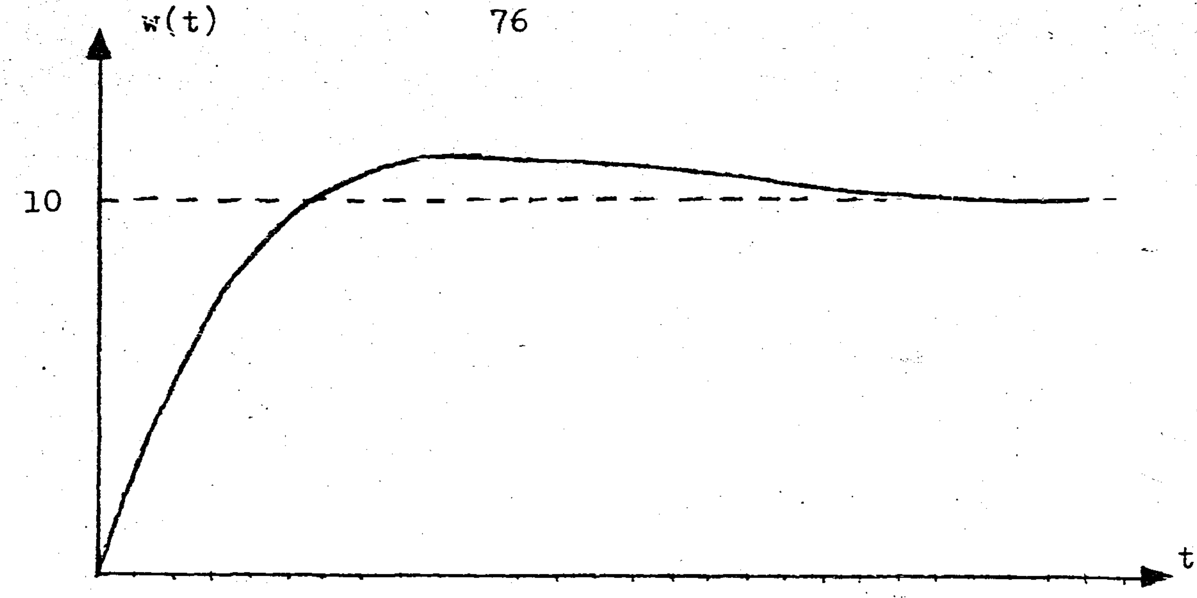

Fig.A.1 PI step response for $K_i = 10$, $K_p = 1.25$
Scale: 16.5msec/div.

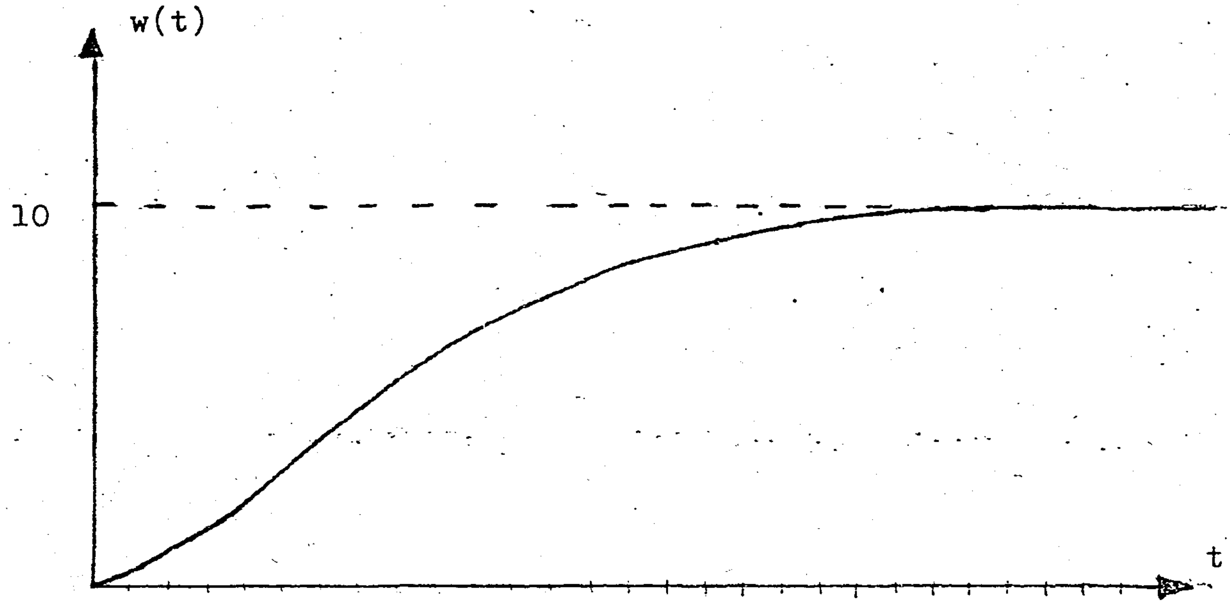

Fig.A.2 IP step response for $K_i=10$, $K_p=1.25$
Scale: 16.5msec/div.

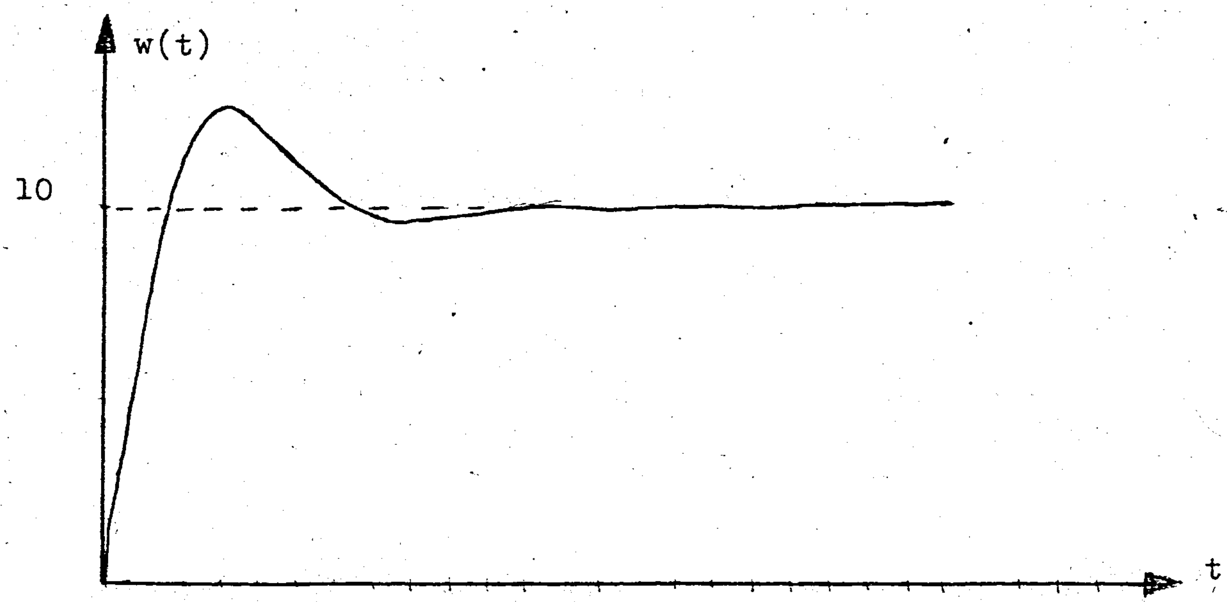

Fig.A.3 PI step response for K_i= 120, K_p= 3
Scale: 16.5msec/div.

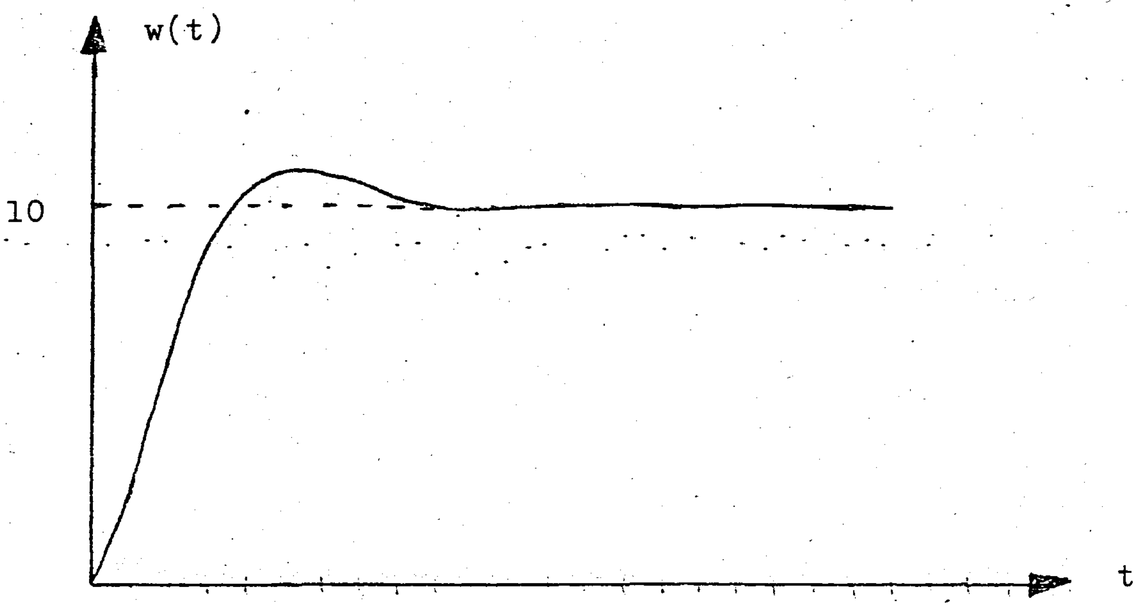

Fig.A.4 IP step response for K_i=120, K_p= 3
Scale: 16.5msec/div.

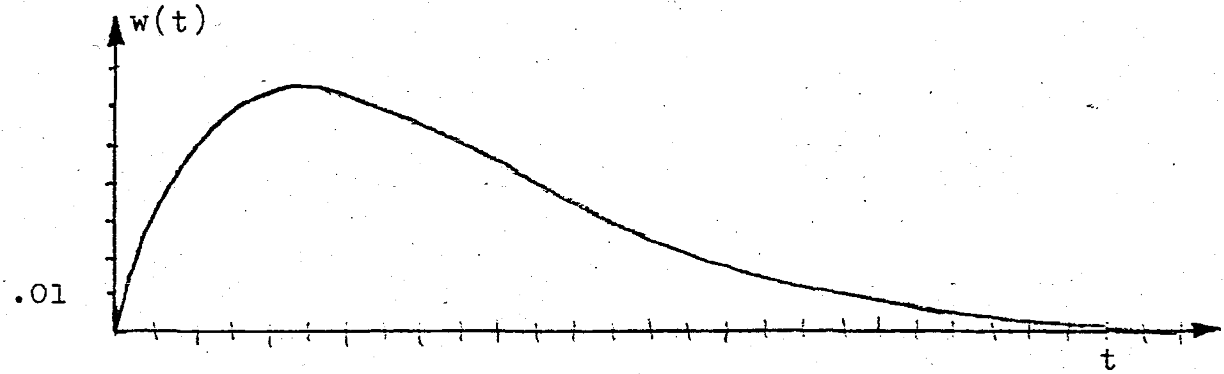

Fig.A.5 Unit step response to the load change for K_i=10, K_p=1.25 ; Time scale: 16.5msec/div.

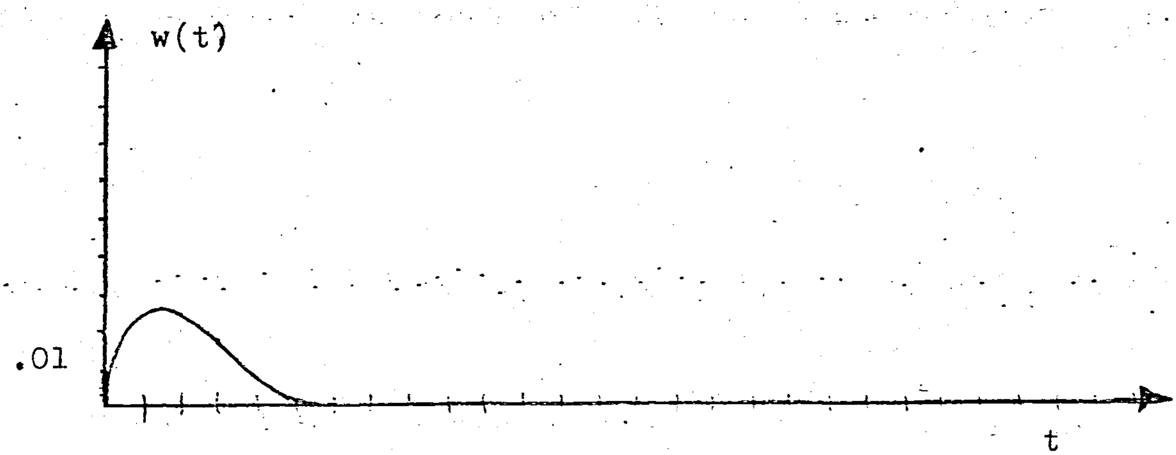

Fig.A.6. Unit step response to the load change for K_i=120, K_p= 3 ; Time scale: 16.5msec/div.

APPENDIX B

....DIGITAL INTEGRAL PROPORTIONAL CONTROLLER....

```
ØØØØ 3EBØ                LD A,BO
ØØØ2 32Ø7EØ              LD (E007H),A
ØØØ5 21ECØ1              LD HL,INTSRV
ØØØ8 22391Ø              LD (1039H),HL
ØØØB DD21ØØ4Ø            LD IX,4000H
ØØØF DD36Ø4Ø6            LD (IX+04H),06
ØØ13 DD36Ø818            LD (IX+08H),18
0017 DD360C0C            LD (IX+0CH),0C
001B DD361021            LD (IX+10H),21
001F DD361403            LD (IX+14H),03
0023 DD361830            LD (IX+18H),30
0027 DD36050C            LD (IX+05H),0C
002B DD360930            LD (IX+09H),30
002F DD360D18            LD (IX+0DH),18
0033 DD361103            LD (IX+11H),03
0037 DD361506            LD (IX+15H),06
003B DD361921            LD (IX+19H),21
003F DD360618            LD (IX+06H),18
0043 DD360A21            LD (IX+0AH),21
0047 DD360E30            LD (IX+0EH),30
004B DD361206            LD (IX+12H),06
004F DD36160C            LD (IX+16H),0C
0053 DD361A03            LD (IX+1AH),03
0057 FD210070            LD IY,7000H
005B DD36215F            LD (IX+33),95
005F DD36225F            LD (IX+34),95
0063 DD36235F            LD (IX+35),95
0067 DD36245E            LD (IX+36),94
006B DD36255D            LD (IX+37),93
006F DD36265D            LD (IX+38),93
0073 DD36275C            LD (IX+39),92
0077 DD36285C            LD (IX+40),92
007B DD36295B            LD (IX+41),91
007F DD362A5A            LD (IX+42),90
0083 DD362B5A            LD (IX+43),90
0087 DD362C59            LD (IX+44),89
          .                         .
          .                         .
          .                         .
01CB DD367D12            LD (IX+125),18
01CF DD367E0F            LD (IX+126),15
01D3 DD367F0C            LD (IX+127),12
01D7 DD218040            LD IX,4080H
01DB DD360008            LD (IX+00),8
01DF DD360102            LD (IX+01),2
01E3 DD360202            LD (IX+2),2
01E7 FB           HLT :  EI
01E8 76                  HALT
01E9 C3E701              JP HLT
01EC F5        INTSRV :  PUSH AF
01ED DB01                IN A,(01H)
01EF 1F                  RRA
01F0 D20802              JP C,FIRE
01F3 1F                  RRA
01F4 D20802              JP NC,MAIN
```

```
01F7 3A6104                     LD A,(ALPHA)
01FA D300                       OUT (00H),A
01FC E67F                       AND 7FH
01FE D300                       OUT (00H),A
0200 CBFF                       SET 7,A
0202 D300                       OUT (00),A
0204 97                         SUB A
0205 D301                       OUT (01H),A
0207 FB                         EI
0208 0E00              MAIN   : LD C,00H
020A ED58                       IN E,(C)
020C DB01                       IN A,(01H)
020E E6C0                       AND C0H
0210 07                         RLCA
0211 07                         RLCA
0212 47                         LD B,A
0213 7B                         LD A,E
0214 E603                       AND 03H
0216 57                         LD D,A
0217 7B                         LD A,E
0218 E6FC                       AND FCH
021A B0                         OR B
021B 5F                         LD E,A
021C ED534904                   LD (INSPD),DE
0220 37                         SCF
0221 3F                         CCF
0222 2A4B04                     LD HL,(SETSPD)
0225 ED52                       SBC HL,DE
0227 DA3102                     JP C,SGNNEG
022A 97                         SUB A
022B 325004                     LD (SGNNER),A
022E C33902                     JP SGNPOS
0231 3E01             SGNNEG  : LD A,01
0233 325004                     LD (SGNNER),A
0236 CDFE03                     CALL NEGATE
0239 7C               SGNPOS  : LD A,H
023A E603                       AND 03H
023C CA4102                     JP Z,ERR8BT
023F 2EFF                       LD L,FFH
0241 2600             ERR8BT  : LD H,00H
0243 225104                     LD (NEWERR),HL
0246 FD7501                     LD (IY+01),L
0249 3A5004                     LD A,(SGNNER)
024C FD7700                     LD (IY+00),A
024F FD23                       INC IY
0251 FD23                       INC IY
0253 FD226304                   LD (TEMP),IY
0257 2A6304                     LD HL,(TEMP)
025A 7D                         LD A,L
025B F600                       OR 00
025D CCBD03                     CALL Z,NEW
0260 2A5104                     LD HL,(NEWERR)
0263 3A4D04                     LD A,(SGNOER)
0266 47                         LD B,A
0267 3A5004                     LD A,(SGNNER)
026A 80                         ADD A,B
026B ED5B4E04                   LD DE,(OLDERR)
026E 0F                         RRCA
```

```
0270 DA8102                        JP C,SDIF1
0273 19                            ADD HL,DE
0274 CD0604                        CALL MULT2
0277 225404                        LD (BETA),HL
027A 78                            LD A,B
027B 325304                        LD (SGBETA),A
027E C3A402                        JP FNDITG
0281 37               SDIF1 :      SCF
0282 3F                            CCF
0283 ED52                          SBC HL,DE
0285 DA9702                        JP C,RESNG1
0288 3A5004                        LD A,(SGNNER
028B 325304                        LD (SGBETA),A
028E CD0604                        CALL MULT2
0291 225404                        LD (BETA),HL
0294 C3A402                        JP FNDITG
0297 CDFE03           RESNG1 :     CALL NEGATE
029A 78                            LD A,B
029B 325304                        LD (SGBETA),A
029E CD0604                        CALL MULT2
02A1 225404                        LD (BETA),HL
02A4 ED5B5704         FNDITG :     LD DE,(OLDITG)
02A8 3A5304                        LD A,(SGBETA)
02AB 47                            LD B,A
02AC 3A5604                        LD A,(SGOITG)
02AF 80                            ADD A,B
02B0 0F                            RRCA
02B1 DAC502                        JP C,SDIF2
02B4 19                            ADD HL,DE
02B5 D2BB02                        JP NC,SUM<FF
02B8 21FFFF                        LD HL,FFFFH
02BB 225A04           SUM<FF :     LD (NEWITG),HL
02BE 78                            LD A,B
02BF 325904                        LD (SGNITG),A
02C2 C3E402                        JP K*CONT
02C5 37               SDIF2 :      SCF
02C6 3F                            CCF
02C7 ED52                          SBC HL,DE
02C9 DAD802                        JP C,RESNG2
02CC 225A04                        LD (NEWITG),HL
02CF 3A5304                        LD A,(SGBETA)
02D2 325904                        LD (SGNITG),A
02D5 C3E402                        JP K*CONT
02D8 CDFE03           RESNG2 :     CALL NEGATE
02DB 225A04                        LD (NEWITG),HL
02DE 3A5604                        LD A,(SGOITG)
02E1 325904                        LD (SGNITG),A
02E4 ED5B5A04         K*CONT :     LD DE,(NEWITG)
02E8 CD3C04                        CALL MULT2
02EB 3A5904                        LD A,(SGNITG)
02EE 0F                            RRCA
02EF D20D03                        JP NC,SDIF3
02F2 19                            ADD HL,DE
02F3 DAFD02                        JP C,OVL
02F6 97                            SUB A
02F7 326204                        LD (OVERLD),A
02FA C30203                        JP Q1
02FD 3E01             OVL :        LD A,01H
```

```
02FF 326204              LD (OVERLD),A
0302 225D04        Q1  : LD (KOUT),HL
0305 3E01                LD A,01H
0307 325C04              LD (SGKOUT),A
030A C32E03              JP DIVIDE
030D 97         SDIF3  : SUB A
030E 326204              LD (OVERLD),A
0311 37                  SCF
0312 3F                  CCF
0313 EB                  EX DE,HL
0314 ED52                SBC HL,DE
0316 DA2303              JP C,RESNG3
0319 225D04              LD (KOUT),HL
031C 97                  SUB A
031D 325C04              LD (SGKOUT),A
0320 C32E03              JP DIVIDE
0323 CDFE03     RESNG3 : CALL NEGATE
0326 225D04              LD (KOUT),HL
0329 3E01                LD A,01H
032B 325C04              LD (SGKOUT),A
032E 0F         DIVIDE : RRCA
032F DA5F03              JP C,N1
0332 3A6204              LD A,(OVERLD)
0335 0F                  RRCA
0336 DA4203              JP C,UPLMT
0339 7C                  LD A,H
033A FE5E                CP 5EH
033C D24203              JP NC,UPLMT
033F C34403              JP LOOKUP
0342 3E5E       UPLMT  : LD A,5EH
0344 2640       LOOKUP : LD H,40H
0346 112100              LD DE,33
0349 6F                  LD L,A
034A 19                  ADD HL,DE
034B 7E                  LD A,(HL)
034C 47         DELAY  : LD B,A
034D E6C0                AND C0H
034F 07                  RLCA
0350 07                  RLCA
0351 326004              LD (RANGE),A
0354 78                  LD A,B
0355 E63F                AND 3FH
0357 F680                OR 80H
0359 326104              LD (ALPHA),A
035C C39003              JP FIN
035F 3A6204        N1  : LD A,(OVERLD)
0362 0F                  RRCA
0363 DA6F03              JP C,UNLMT
0366 7C                  LD A,H
0367 FE40                CP 40H
0369 D26F03              JP NC,UNLMT
036C C37103              JP REGN
036F 3E3F       UNLMT  : LD A,3FH
0371 47         REGN   : LD B,A
0372 3E60                LD A,60H
0374 80                  ADD A,B
0375 47                  LD B,A
0376 E60F                AND 0FH
```

```
0378 CA8B03                    JP Z,CORECT
037B 78                        LD A,B
037C FE80            RLMT  :   CP 128
037E D24C03                    JP NC,DELAY
0381 FE7B                      CP 123
0383 DA4C03                    JP C,DELAY
0386 3E7B                      LD A,123
0388 C34C03                    JP DELAY
038B 78            CORECT  :   LD A,B
038C 3C                        INC A
038D C37C03                    JP RLMT
0390 2A5104           FIN  :   LD HL,(NEWERR)
0393 224E04                    LD (OLDERR),HL
0396 3A5004                    LD A,(SGNNER)
0399 324D04                    LD (SGNOER),A
039C 2A5A04                    LD HL,(NEWITG)
039F 225704                    LD (OLDITG),HL
03A2 3A5904                    LD A,(SGNITG)
03A5 325604                    LD (SGOITG),A
03A8 CD1E00                    CALL BRKEY
03AB CA1B04                    JP Z,MODIFY
03AE CDC203                    CALL SPCHNG
03B1 CA0B04                    JP Z,PCHNG
03B4 CDE003                    CALL SNCHNG
03B7 CC1404                    CALL Z,NCHNG
03BA F1              BACK  :   POP AF
03BB ED4D                      RETI
03BD FD210070         NEW  :   LD IY,7000H
03C1 C9                        RET
03C2 3EF8          SPCHNG  :   LD A,F8
03C4 3200E0                    LD (E000),A
03C7 00                        NOP
03C8 3A01E0                    LD A,(E001)
03CB 2F                        CPL
03CC E621                      AND 21H
03CE C2D403                    JP NZ,2NDP
03D1 C601                      ADD A,01
03D3 C9                        RET
03D4 3EF2            2NDP  :   LD A,F2
03D6 3200E0                    LD (E000),A
03D9 00                        NOP
03DA 3A01E0                    LD A,(E001)
03DD E604                      AND 04
03DF C9                        RET
03E0 3EF8          SNCHNG  :   LD A,F8
03E2 3200E0                    LD (E000),A
03E5 00                        NOP
03E6 3A01E0                    LD A,(E001)
03E9 2F                        CPL
03EA E621                      AND 21H
03EC C2F203                    JP NZ,2NDN
03EF C601                      ADD A,01
03F1 C9                        RET
03F2 3EF4            2NDN  :   LD A,F4
03F5 3200E0                    LD (E000),A
03F7 00                        NOP
03F8 3A01E0                    LD A,(E001)
03FB E604                      AND 04
```

```
03FD C9                          RET
03FE 7D             NEGATE   :   LD A,L
03FF 2F                          CPL
0400 6F                          LD L,A
0401 7C                          LD A,H
0402 2F                          CPL
0403 67                          LD H,A
0404 23                          INC HL
0405 C9                          RET
0406 00              MULT2   :   NOP
0407 00                          NOP
0408 00                          NOP
0409 00                          NOP
040A C9                          RET
040B 216002          PCHNG   :   LD HL,0260H
040E 224B04                      LD (SETSPD),HL
0411 C3BA03                      JP BACK
0414 212002          NCHNG   :   LD HL,0220H
0417 224B04                      LD (SETSPD),HL
041A C9                          RET
041B 214124         MODIFY   :   LD HL,2441H
041E 223910                      LD (1039H),HL
0421 C30060                      JP BRK
0424 D9               FIRE   :   EXX
0425 DB01                        IN A,(01H)
0427 CB6F                        BIT 5,A
0429 CA3804                      JP Z,CRLIMT
042C E61C                        AND 1C
042E 216004                      LD HL,RANGE
0431 B6                          OR (HL)
0432 6F                          LD L,A
0433 2640                        LD H,40H
0435 7E                          LD A,(HL)
0436 D301                        OUT (01),A
0438 D9             CRLIMT   :   EXX
0439 F1                          POP AF
043A ED4D                        RETI
043C 2A4904                      LD HL,(INSPD)
043F 29                          ADD HL,HL
0440 29                          ADD HL,HL
0441 29                          ADD HL,HL
0442 29                          ADD HL,HL
0443 00                          NOP
0444 00                          NOP
0445 00                          NOP
0446 00                          NOP
0447 00                          NOP
0448 C9                          RET
0449 0000            INSPD   :   DEFW
                    SETSPD   :   DEFW
                    SGNOER   :   DEFB
                    OLDERR   :   DEFW
                    SGNNER   :   DEFB
                    NEWERR   :   DEFW
                    SGBETA   :   DEFB
                    BETA     :   DEFW
                    SGOITG   :   DEFB
                    OLDITG   :   DEFW
```

```
SGNITG  : DEFB
NEWITG  : DEFW
SGKOUT  : DEFB
KOUT    : DEFW
RNG     : DEFB
RANGE   : DEFB
ALPHA   : DEFB
OVERLD  : DEFB
TEMP    : DEFW
BRK     : EQU   6000H
BRKEY   : EQU   001E
          END
```

APPENDIX C

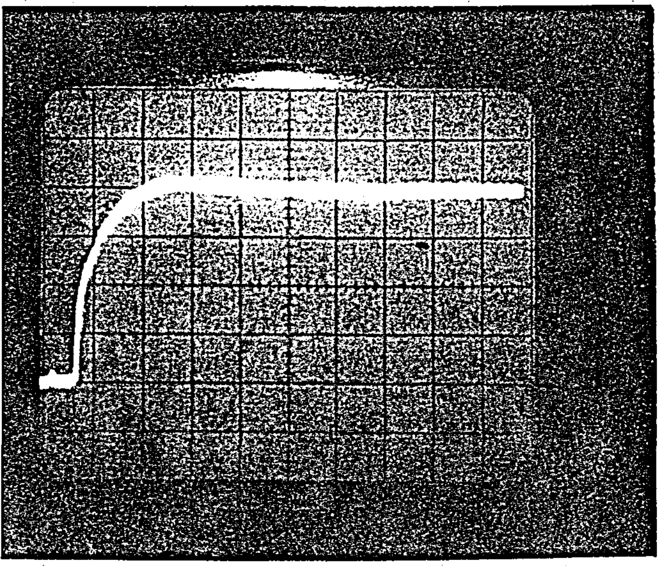

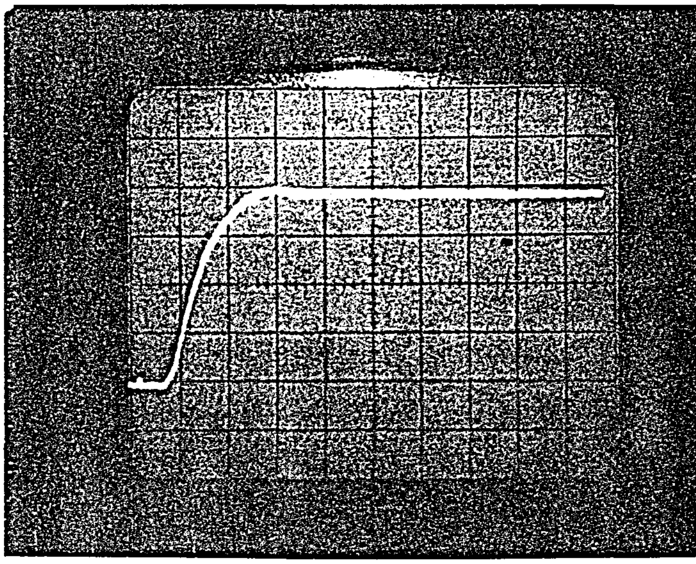

(a) (b)

$K_i=10$, $K_p=1.25$; Scale: .5sec/cm , .5V/cm

Change of speed: 200rpm

Photo.1 (a) PI step response; (b) IP step response.

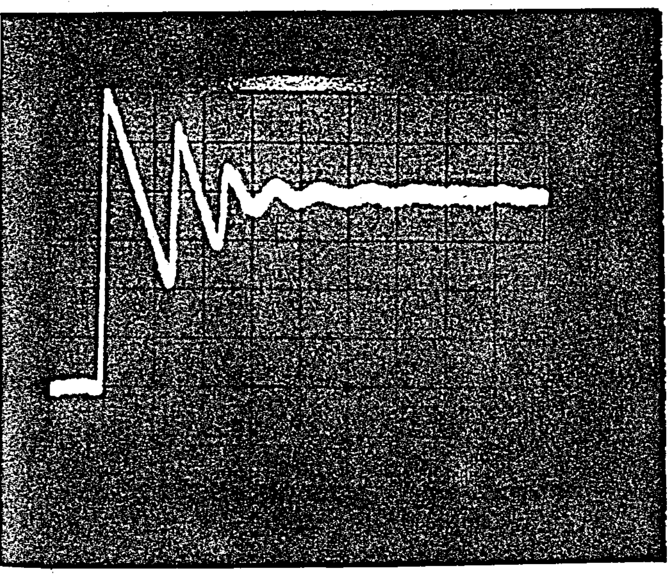

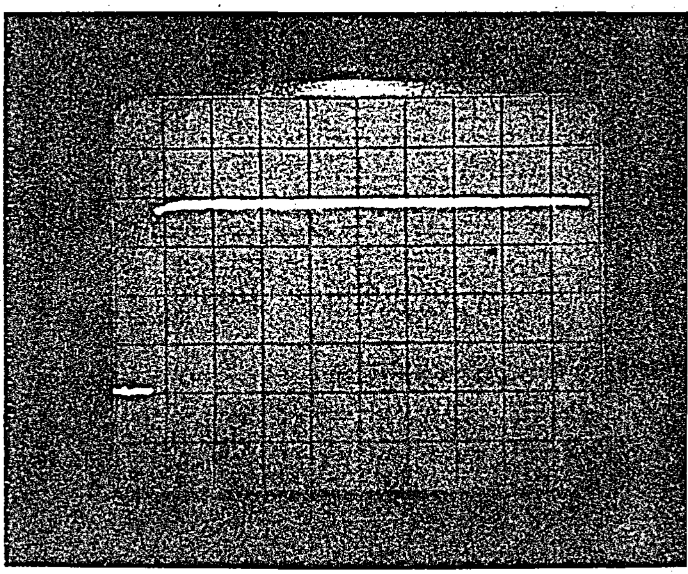

(a) (b)

$K_i=120$, $K_p=3$; Scale: .5sec/cm, .5V/cm

Change of speed: 200rpm

Photo.2 (a) PI step response (b) IP step response.

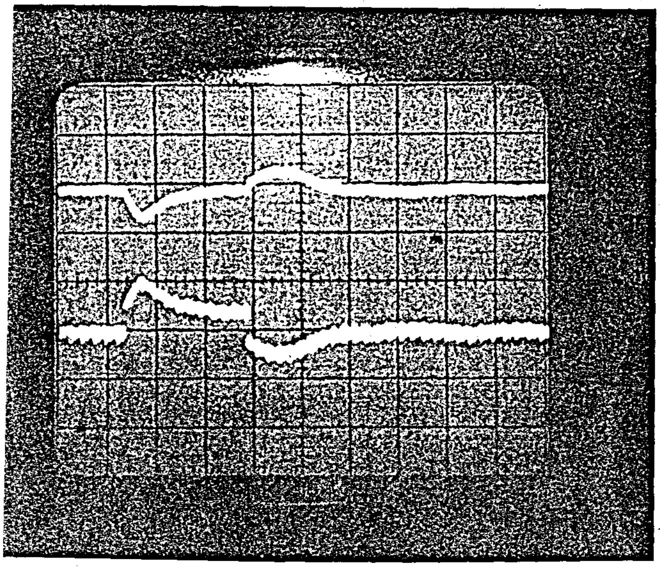

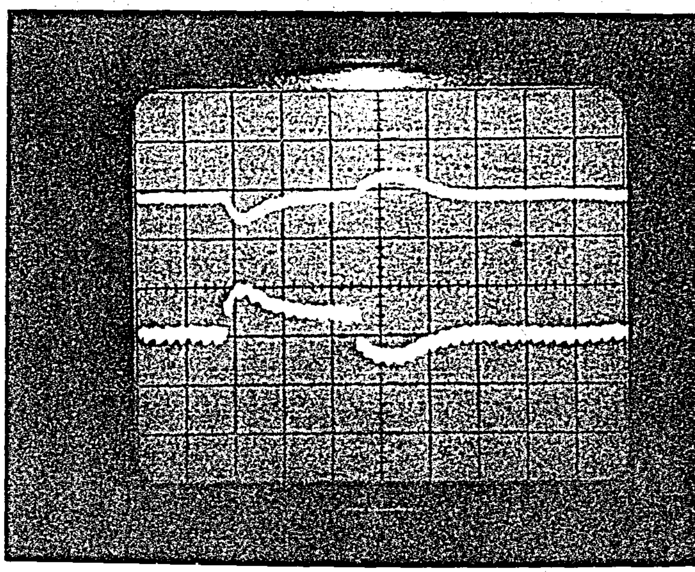

(a) (b)

K_i=10, K_p=1.25 ; Scale: .2V/cm=25rpm, .5sec/cm

Photo.3 (a) PI change of load (b) IP change of load.

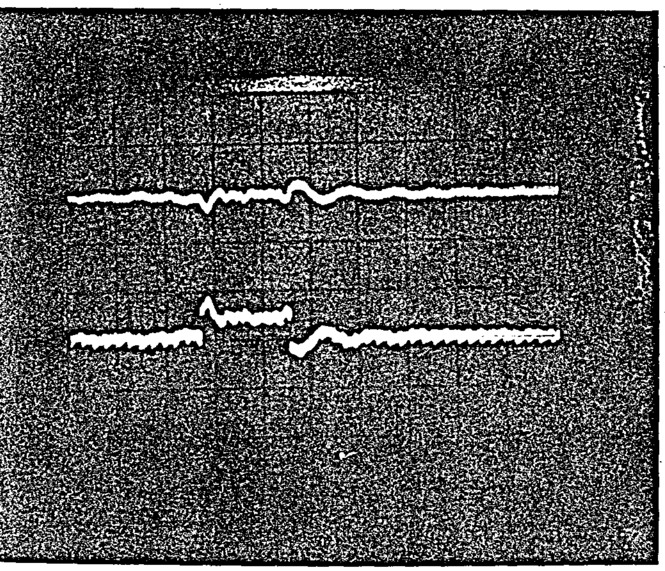

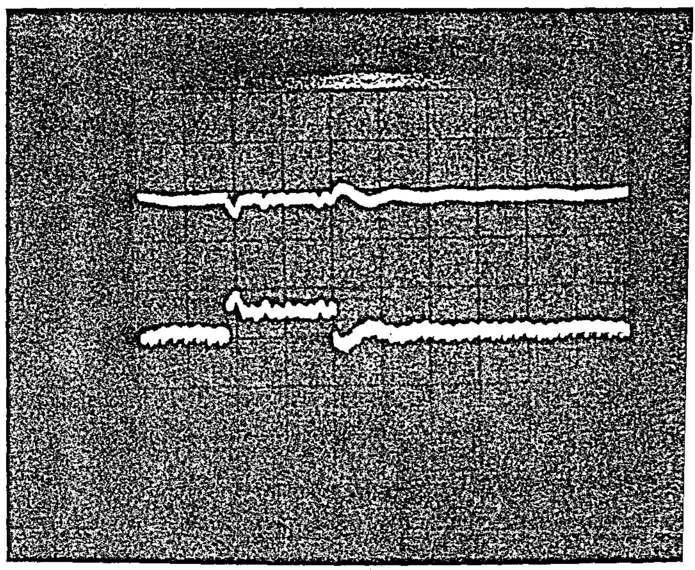

(a) (b)

K_i=120, K_p=3 ; Scale: .2V/cm=25rpm, .5sec/cm

Photo.4 (a) PI change of load (b) IP change of load.

APPENDIX D

CONNECTIONS OF THE BOXES

A. Small Box

Interface between the μP and the bridge.

1. Front Panel

A/D input :

+ which should not exceed +10V

- it is grounded inside

2. Back

+5V O

-5V O

G O

Yellow	Blue	Green
O	O	O
V_a	V_b	V_c

match the same colours of the cables

O +15V Green wire

O -15V White wire

Brown wire is ground which should be connected to the system ground.

(∓ 15V power supply which is inside the big box is fed by 220V~)

3. Gate Pulses

Colours should match at the blue socket

1 Purple	4 Brown
2 Red	5 White
3 Green	6 Yellow

B. I/O PORTS

1. Output ØØ

7	6	5	4	3	2	1	0
Load signal	Empty	Counter					

2. Output Ø1

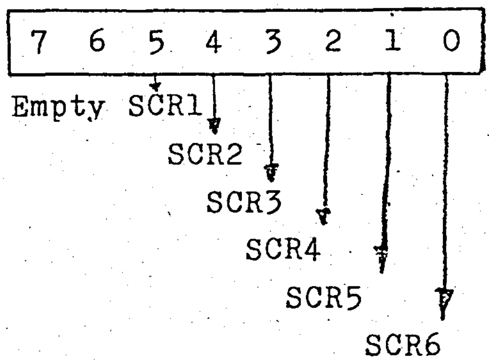

3. Input ØØ

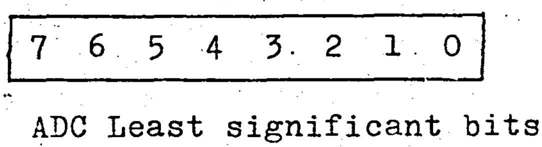

4. Input Ø1

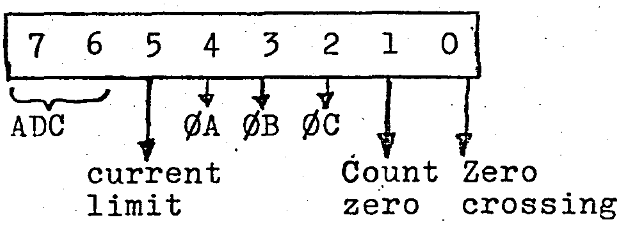

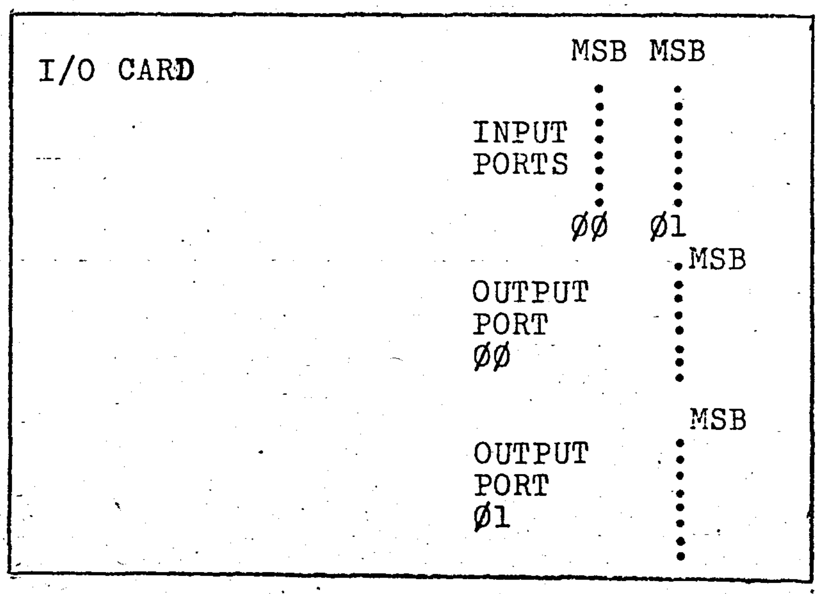

C. I/O SOCKET

1	2	3	4	5	6	7	8	9	10	11	12	13	14
Ld	NC												

Count values   Gate pulses

15	16	17	18	19	20	21	22	23	24	25	26	27	28	29	30
ZC	CZ	Øc	Øb	Øa	CL										

ADC

31
Base interrupt
which goes to the
breadboard by a grey wire

D. Thyristor Bridge Box

It contains six thyristors and pulse transformers together with the corresponding transistors. There is also a current limiting resistor(0.35Ω/5W).

The switch inside the box breaks the power(+15V) going to the pulse transformers. This switch protects the microcomputer from loading all ones during initialization. After the system has been run, this switch must be closed

Blue switch cuts the three phase mains from the thyristors.

E. OPERATING THE SYSTEM

Load the Symbolic Debugger

Load the program

Connect ∓15V power supply to the mains

Connect ∓5V to the small box

Close the three phase

Set a break point to the address location of 6ØØØH

Run the program

Close the three phase mains switch(at the right side of the bridge box

Close the pulse transformer switch

Now the system must operate

Shift+T speed increase

Shift+G speed decrease

F. Stopping the System

Press shift+break keys

or

Open the three-phase mains switch

or

Open the pulse transformer switch

G. Current Limit

The output of the current limiting circuit is normally Logic '1', and becomes Logic '0' when the current passing through the motor exceeds approximately 6A.

4ØØØH-4Ø1AH addresses contain Firing Look-up Table

4Ø21H-4Ø82H addresses contain Inverse Cos. Table.

APPENDIX E

SEPARATELY EXCITED DC MOTOR

DC motors are widely used in industrial speed control drives. In modern dc drives, the classical motor-generator set has been replaced by a thyristorized power converter which provides faster response at a lower cost. To obtain the necessary speed accuracy, closed loop control is usually necessary. Closed or feedback systems generally have the advantages of greater accuracy, improved dynamic response, and reduced effect of disturbances such as loading.

With solid-state power controllers, protection can be an important consideration. For simplicity and ease of understanding, the system is reduced to the lowest possible order. This requires neglecting some smaller time constants.

Consider the separately excited dc motor with armature voltage shown in Figure.3.C.4. The voltage loop equation is

$$e_a = e_g + i_a R_a + di_a/dt\ L_a \qquad (3.D.11)$$

where

$$e_g = k_a \phi w \qquad (3.D.12)$$

The torque balance equation is

$$T_e = T_L + Bw + J\ dw/dt \qquad (3.D.13)$$

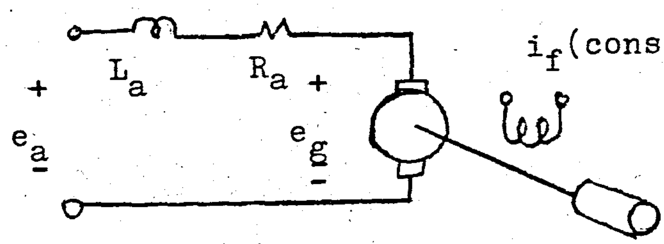

(a)

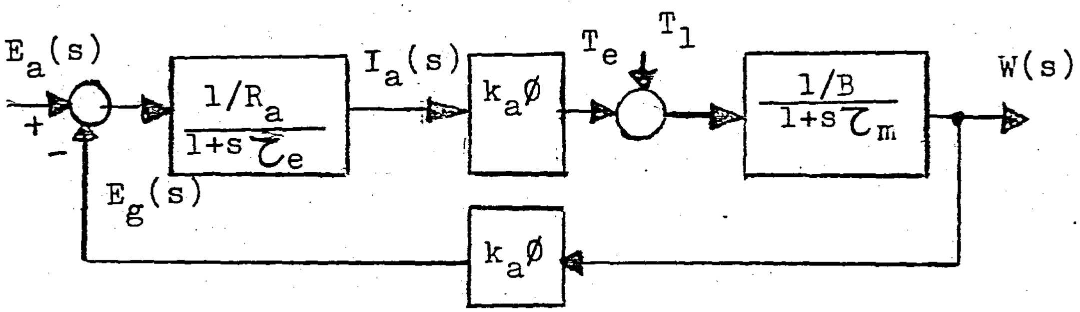

(b)

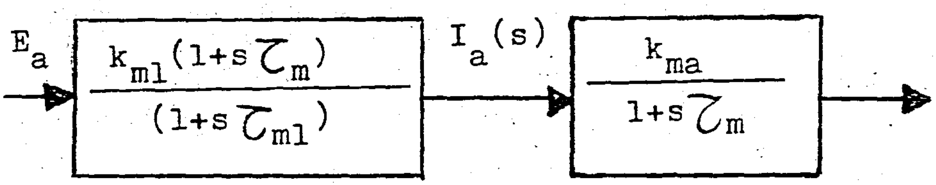

(c)

Fig.3.C.4 Development of motor transfer function (a) separately excited dc model, (b) complete transfer function, (c) simplified transfer function.

where

$$T_e = k_a \emptyset i_a \qquad (3.D.14)$$

In the laplace domain, Eq. (3.D.11-14) can be written as

$$E_a(s) = E_g(s) + R_a I_a(s) + L_a s I_a(s) \qquad (3.D.15)$$

$$E_g(s) = k_a \emptyset W(s) \qquad (3.D.16)$$

$$T_e(s) = T_L(s) + BW(s) + JsW(s) \qquad (3.D.17)$$

$$T_e(s) = k_a \emptyset I_a(s) \qquad (3.D.18)$$

Thus

$$I_a(s)=\frac{E_a(s)-E_g(s)}{R_a+sL_a}=\frac{(E_a(s)-E_g(s))/R_a}{1+\tau_e s}$$

where

$$\tau_e=L_a/R_a$$

$$W(s)=\frac{T_e(s)-T_L(s)}{B+Js}=\frac{(T_e(s)-T_L(s))/B}{1+\tau_m s}$$

where

$$\tau_m=J/B$$

These relationships are shown in block diagram form in Figure.3.C.4b

Note the feedback loop present in the form of the back EMF. This provides the moderate speed regulation inherent in the separately excited dc motor.

From Figure.3.C.4b , an expression can be obtained for the change in speed W(s) because of disturbances in applied voltage, $E_a(s)$, and load torque, $T_L(s)$.

$$W(s)=\frac{G_1(s)}{1+G_1(s)H_1(s)}E_a(s)+\frac{G_2(s)}{1+G_2(s)H_2(s)}T_L(s)$$

where

$$G_1(s)=\left(\frac{1/R_a}{1+s\tau_e}\right)(k_a\phi)\left(\frac{1/B}{1+s\tau_m}\right),\quad H_1(s)=k_a\phi$$

$$G_2(s)=\frac{-1/B}{1+s\tau_m}, \quad H_2(s)=\frac{-(k_a\phi)^2/R_a}{1+s\tau_m}$$

If we neglect the load torque term for now,

$$\frac{W(s)}{E_a(s)}=\frac{k_a\phi}{(k_a\phi)^2+R_aB(1+s\tau_e)(1+s\tau_m)}$$

If $\tau_e \ll \tau_m$ (which is almost always the case), then τ_e can be neglectted and the expression simplifies to

$$\frac{W(s)}{E_a(s)}=\frac{k_a\phi}{(k_a\phi)^2+R_aB+sR_aB\tau_m}=\frac{k_m}{1+s\tau_{m1}}$$

where

$$\tau_{m1}=\frac{R_aB}{(k_a\phi)^2+R_aB}\tau_m, \quad k_m=\frac{k_a\phi}{(k_a\phi)^2+R_aB}, \quad \tau_{m1}<\tau_m$$

Referring to Figure.3.C.4b

$$\frac{W(s)}{I_a(s)}=\frac{k_a\phi/B}{1+s\tau_m}$$

Therefore,

$$\frac{I_a(s)}{E(s)}=\frac{W(s)}{E_a(s)}\times\frac{I_a(s)}{W(s)}$$

$$= \frac{k_m}{k_a\emptyset/B} \frac{(1+s\tau_m)}{(1+s\tau_{m1})}$$

The motor can then be represented, for voltage control analysis purposes, as two blocks as in Figure.3.C.4c where

$$k_{m1} = \frac{B}{(k_a\emptyset)^2 + R_a B} \quad , \quad k_{m2} = \frac{k_a\emptyset}{B} \quad , \quad k_m = k_{m1}k_{m2}$$

In the proceeding analysis, we will define τ_{m1} as T_m for simplicity.

Resulting discrete state equations are as follows:

$$\begin{bmatrix} x_1((k+1)T) \\ x_2((k+1)T) \end{bmatrix} = \begin{bmatrix} \exp(-T/T_m & 0 \\ T_m(1-\exp(-T/T_m) & 1 \end{bmatrix} \begin{bmatrix} x_1(kT) \\ x_2(kT) \end{bmatrix} + \begin{bmatrix} K_m(1-\exp(-T/T_m) \\ K_m(T-T_m(1-\exp(-T/T_m) \end{bmatrix} u(kT)$$

$$y(kT) = x_1(kT)$$

BIBLIOGRAPHY

1. F. Harashima et al, "Performance Improvement in Microprocessor-Based Digital PLL Speed Control System", IEEE Trans.,Vol.IECI-28,No.1,pp56-61;Feb.1981

2. F. Harashima and S. Kondo,"Microprocessor-Based Optimal Speed Control System of Motor Drives", IEEE 1981 IECI Proceedings.

3. D.B. Izosimov and V.I. Utkin,"Sliding Mode Control of Electric Motors", Preprints of IFAC 8th World Cong.1, Kyoto Japan, Vol. XVII,pp 13-19,1981.

REFERENCES NOT CITED

James A. Cadzow. Discrete-Time and computer control systems. Prentice-Hall,Inc. 1970.

Ogata K. Medern Control Engineer ng. Rpentice-Hall International Inc. 1970

Ogata K. State Space Analysis of Control Systems. Prentice-Hall,Inc.,Englewood Cliffs,N.J.,1967.